Design and synthesis of 1-((1,5-bis(4-chlorophenyl)-2-methyl-1H-pyrrol-3-yl)methyl)-4-methylpiperazine (BM212) and *N*-Adamantan-2-yl-*N*'-((E)-3,7-dimethyl-octa-2,6-dienyl)-ethane-1,2-diamine (SQ109) pyrrole hybrid derivatives: discovery of potent anti-tubercular agents effective against multi-drug resistant mycobacteria

Sanjib Bhakta,[a,¶] *Nicolò Scalacci,*[b,e] *Arundhati Maitra,*[a] *Alistair K. Brown,*[f,b] *Saiprasad Dasugari,*[b] *Dimitrios Evangelopoulos,*[c,‡] *Timothy D. McHugh,*[c] *Parisa N. Mortazavi,*[a] *Alexander Twist,*[b] *Elena Petricci,*[d] *Fabrizio Manetti,*[d,¶,*] *and Daniele Castagnolo.* [e, b, ¶,*]

[a]Mycobacteria Research Laboratory, Department of Biological Sciences, Institute of Structural and Molecular Biology, Birkbeck, University of London, Malet Street, London WC1E 7HX, UK. [b]Department of Applied Sciences, Northumbria University Newcastle, Ellison Place, NE1 8ST, Newcastle upon Tyne, UK. [c]Centre for Clinical Microbiology, University College London, London, NW3 2PF, UK. [d]Dipartimento di Biotecnologie, Chimica e Farmacia, via A. Moro 2, I-53100 Siena, Italy. [e]Institute of Pharmaceutical Science, King's College London, 150 Stamford Street, London SE1 9NH, UK. [f]School of Medicine, Pharmacy and Health, Durham University, Queen's Campus, Stockton-on-Tees, TS17 6BH, UK.

KEYWORDS. Tuberculosis, MDR-TB, Antimicrobial resistance, BM212, SQ109, efflux pump, pyrrole, HT-SPOTi, common feature hypothesis generation approach

ABSTRACT. Novel pyrroles have been designed, synthesized and evaluated against mycobacterial strains. The pyrroles have originally been designed as hybrids of the anti-tubercular drugs BM212 **1** and SQ109 **2** that showed common chemical features with very similar topological distribution. A perfect superposition of the structures of **1** and **2** revealed by computational studies suggested the introduction of bulky substituents at the terminal portion of the pyrrole C3 side chain and the removal of the C5 aryl moiety. Five compounds showed high activity toward *Mycobacterium tuberculosis*, while **9b** and **9c** were highly active also against multi-drug resistant clinical isolates. Compound **9c** showed low eukaryotic cell toxicity, turning out to be an excellent lead candidate for preclinical trials. In addition, four compounds showed potent inhibition (comparable to that of verapamil) towards the whole-cell drug efflux pump activity of mycobacteria, and thus turning to be promising multi-drug resistance reversal agents.

INTRODUCTION

Tuberculosis (TB) was first declared as a global health emergency by the World Health Organisation (WHO) in 1993. More than two decades on, the world is still grappling to control the spread of this infectious disease. In 2014, around 9.3 million people were estimated to have fallen ill with TB and 1.5 million deaths were caused by it.[1] Although, mortality due to TB has fallen to 47% since 1990, the increasing resistance seen in the TB-causative organism, *Mycobacterium tuberculosis* (MTB), is responsible for new 480,000 estimated cases of multidrug-resistant TB. In fact, multi-, extensively- and even totally-drug resistant tuberculosis (MDR-,[2-4] XDR-,[5-6] TDR-TB[7]) cases make the disease, originally difficult to treat, even more so as most drugs in use today are ineffective to treat these mutant strains. Moreover, two billion people are estimated to be latently infected with MTB, and 10% of them reactivate to active TB with major risk relative to immigrants from endemic areas, people with HIV-1 infection, and individuals with underlying diseases (e.g. silicosis, diabetes mellitus and malignant conditions). Treatment, if available, is lengthy, severely toxic and prone to interfere with other therapies such as the antiretroviral therapy in the case of TB-HIV co-infected patients.

The need for new shorter therapeutic regimens and new classes of drugs active against MDR-, XDR-, and TDR-TB drives pharmaceutical research to accelerate in the development process of new anti-TB drugs. There is an urgent need to develop novel anti-tubercular agents with alternative mechanisms of action to control TB, one of the leading causes of mortality due to a single infectious agent.

About fifteen years ago, the pyrrole compound **1** (BM212)[8] was discovered to be a potent anti-mycobacterial agent. In an effort to identify new pyrrole analogues with improved solubility and

ability to kill MDR and XDR mycobacteria, many derivatives of **1** were designed and synthesized.[8-10] Congeners of **1** showed a micromolar activity toward MTB H37Rv. However, the first series of analogues (including **1** itself) suffered from poor pharmacokinetic parameters (in terms of clearance and microsomal stability) and significant cytotoxicity. Although the most recent derivatives showed an improved pharmacokinetics and cytotoxicity profile, their physicochemical parameters (such as lipophilicity and aromaticity) need further optimization.[11] Genetic analyses of spontaneous mutants resistant to **1** led to the identification of its cellular target as the trehalose monomycolate exporter, MmpL3 protein (Rv0206c), member of MmpL (Mycobacterial membrane protein Large) family and a validated drug target in MTB.[12] This family has primary structure homology to the resistance-nodulation-cell division (RND) protein family, mainly involved in drug resistance in Gram-negative bacteria.[11] Although the MTB genome encodes 13 members of the MmpL family, their function has not been clearly elucidated. Despite their annotation as multi-drug transporters, they do not contribute to anti-mycobacterial drug resistance.[13] MmpL3 has also been implicated in heme acquisition by MTB, although it might not be its primary role in an endogenous environment.

Adamantane-diamine compound **2** (SQ109) [14] was described as an anti-tubercular drug which is active against susceptible and drug resistant MTB strains. Compound **2** exhibited promising activity in drug combination during animal preclinical studies[15] but also experienced poor pharmacokinetic parameters.[16] Diamine **2** is currently undergoing phase 2 clinical trials for further development.[17] Anti-mycobacterial activity of both **1** and **2** was demonstrated to derive from targeting the MmpL3 protein.[12] Given the ability of **1** and **2** to act as anti-mycobacterial agents through a common molecular target, we pursued the hypothesis that they could share common molecular portions.

By means of an *in silico* molecular modelling approach, the three-dimensional structure of both compounds was studied. Although the apparent structural dissimilarity between the two compounds, a rough comparison of the molecular structures of **1** and **2** showed an unexpected similarity of the topological distribution of their chemical features (Figure 1). In fact, apart from the terminal adamantyl moiety of **2** and the *p*-Cl phenyl ring at the C5 position of **1**, the remaining part of the structure of **2** was superposable to that of **1**.

On the basis of this similarity, we chose to apply a molecular hybridization approach to design new putative anti-mycobacterial compounds.

The molecular hybridization approach is one of the strategies included within the rational design protocol for identification of new biologically relevant small molecules. This approach is based on the recognition of structurally comparable or similar molecular portions of two or more bioactive compounds. By means of merging of these molecular portions, new hybrid chemical entities that maintain structural elements of the parent compounds could be designed. In this study, we have chosen the more rigid scaffold of **1** as the template, and to adjust it upon comparison with the flexible structure of **2**. As a result, the *N*-(substituted)phenyl pyrrole core of **1** with a piperazinyl-methyl side chain at position C3 was maintained, while the second phenyl substituent at position C5 of **1** was deleted from the new hybrid compounds. In addition, the adamantyl moiety present in **2** was inserted as the terminal group bound to N4 of the piperazine ring leading to the design of the hybrid compound **A** (Figure 1).

Hence, we designed, synthesised and biologically evaluated a set of novel pyrrole derivatives with general structure **A** that are hybrid compounds of the anti-tubercular agents **1** and **2**. To explore the chemical space around the C3 piperazino-methyl moiety of the new compounds, the

distal piperazine nitrogen is substituted with different bulky R^2 moieties, such as adamantyl, norbornyl, cyclohexyl, or aryl groups. Moreover the role of the substituent on C5 and its importance for the anti-tubercular activity was explored. According to our superposition hypothesis, the aryl moiety at C5 of **1** was replaced by a methyl substituent, thus leading to design a library of 2,5-dimethylpyrroles. In addition, a second series of simplified derivatives **B** was also designed through molecular simplification in order to evaluate the influence of the piperazine ring on the anti-tubercular activity. Within this series, also according to previous works,[18-19] the piperazine ring was removed from the structure and replaced with a secondary amine (or hydroxylamine) at C3. In both cases, the methyl substituent at C2 and C5, as well as the N1 aryl groups were left unchanged.

RESULTS

Computational design and hypothesis on the common chemical features shared by 1 and 2: To confirm the superposition pattern above described for **1** and **2**, the Phase software[20] was used to find the three-dimensional arrangements of the common chemical portions shared by the two compounds (thereafter referred to as common feature models or superposition models). As a result, a four-feature representation was obtained, comprised of two hydrophobic groups and two protonable atoms (Figure 2). In detail, the *p*-Cl group at the N1 position of the pyrrole ring of **1** and one of the terminal methyl group of **2** matched one of the common hydrophobic regions (H6). The central methyl group of **2** and the 2-methyl group of **1** corresponded to the second hydrophobic portion (H4). On the other hand, the two positively ionizable features (P7 and P8) accommodated the two basic nitrogen atoms of both compounds.

It is important to point out that this representation of the common chemical features of **1** and **2** showed two protonable sites that are chemically unrealistic at neutral pH. However, this qualitative model only accounts for the presence of the two piperazine nitrogens of **1** and for the two amine nitrogens of **2**, while it does not take into consideration the mutual influence of the two amines during the protonation steps. This limitation was eliminated in a second generation, optimized common feature model that is characterized by only one protonable group (Figure 3).

Analysis of the superposition pattern of **1** and **2** prompted us to omit the aromatic portion at position 5 of **1**. In fact, a visual inspection of the superposed structures of **1** and **2** showed that this moiety does not match an analogous group on **2** (Figure 2), and, consequently, it does not represent a common feature of both compounds. Moreover, since the three aromatic rings forced the structure of these compounds toward planarity, the removal of one or more of them could be in principle profitable for better solubility and bioavailability. In addition, given the well-established relationship between late stage drug development problems (i.e., the high attrition rate of compounds entering the clinical phase) and lipophilicity of compounds,[21-22] modulation of lipophilicity should be taken into account when new putative anti-mycobacterial compounds are designed. In addition, since the terminal methyl group of **1** is partially superposed to the adamantyl moiety of **2**, a hydrophobic group at this position was maintained. Following these suggestions and taking into account the similarity between **1** and **2**, a new class of pyrrole derivatives was designed on the basis of the molecular hybridization routine with the aim of obtaining new putative anti-mycobacterial compounds.

The rigid scaffold of **1** was thus chosen as the template for the design of novel antitubercular compounds, and this choice was mainly based on the fact that our research group is well

experienced in the synthesis of pyrrole compounds. Moreover, the adamantyl group already found in **2** was introduced on the piperazine ring, while the 5-phenyl ring of **1** was removed.

Chemistry: *Synthesis of derivatives with general structure A.* A library of pyrrole derivatives bearing an *N*-substituted piperazino-methyl chain at C3 was first synthesized according to classical synthetic procedures. Pyrroles **3a-e** were synthesized through a microwave-assisted Paal-Knorr reaction starting from the appropriate diones and different anilines.[18, 23-24] Despite computational studies suggested to keep a *p*-Cl moiety fixed on the N1 aryl group, a number of different substituents was also introduced to evaluate their steric and electronic effects on the anti-mycobacterial activity and to deduce SAR considerations. Pyrroles **3a-e** were then coupled with differently substituted piperazines in the presence of formaldehyde to afford desired pyrroles **7a-m** (Table 1). Different bulky substituents were introduced on the piperazine ring to explore the chemical space around the pyrrole nucleus. The piperazines **6c-e** (cyclohexyl-piperazine **6c**, phenyl-piperazine **6d**, 1-adamantyl-piperazine **6e**) are commercially available and were coupled with **3a-e** as purchased. The piperazines **6a-b** were synthesized as described in Scheme 1 and then reacted with the pyrroles **3a-e**. The Boc-piperazine **4** and the appropriate ketones **5a-b** (2-adamantanone **5a**, 2-norbornanone **5b**) were reacted in the presence of the reducing agent $Na(OAc)_3BH$ to yield the corresponding alkylpiperazine intermediates, which were immediately converted into the desired piperazines **6a-b** by TFA-mediated Boc-cleavage. Piperazines **6a-e** and pyrroles **3a-e** were then coupled *via* Mannich reaction to afford pyrroles **7a-m** (Table 1).

Synthesis of derivative with general structure B. A second series of pyrrole derivatives with general structure **B** was synthesised as described in Scheme 2. Pyrrole **3a-c** were formylated through Vilsmeir-Haack reaction affording the aldehydes **8a-c**. The latter compounds were

reacted with different primary amines in the presence of $Na(AcO)_3BH$ to yield pyrroles **9a-j**. Moreover, aldehydes **8a-b** were reacted with benzylhydroxylamine to afford oximes **10a-b**[18] which, after treatment with $NaCNBH_3$, led to the corresponding hydroxylamines **11a-b** in excellent yields.

Biology: All the compounds were tested for their biological activity by determining the minimum inhibitory concentrations (MIC) against a panel of fast-growing environmental and slow-growing mycobacterial species and clinical isolates (Table 3 and 4). This included the fast-growing non-pathogenic strains of *M. smegmatis* and relatively fast-growing intracellularly surviving *M. aurum*[25] followed by the vaccine strain *M. bovis* BCG, the non-pathogenic *M. tuberculosis* mc^27000, and finally the pathogenic *M. tuberculosis* H37Rv. Furthermore, we also tested the activity of these compounds against MDR-TB clinical isolates. In addition, cytotoxicity analysis was carried out. The eukaryotic cell toxicity of each compound was tested against murine macrophage RAW264.7 cells and human monocyte-derived THP-1 cell line to ascertain the 50% growth inhibitory concentration (GIC_{50}). Mouse models are routinely used for testing the efficacy of both anti-tubercular drugs and vaccines and are considered a highly appropriate model. In particular, RAW264.7 are differentiated macrophage cells capable of eliciting a whole host of inflammatory responses and been studied and characterised in great detail over many decades.[26] The ratio of the MIC observed against MTB H37Rv and the GIC_{50} values provided the selectivity index (SI), or the therapeutic window offered by these molecules. It must to be brought to note that there are differences in the assay methods to determine the inhibitory concentrations of the compounds against the bacterial pathogen and the eukaryotic cells. However, these methods have been extensively standardised so as to reduce ambiguity in inferring the selectivity index from these assays. Finally, the effect of these compounds on the

efflux pump activity of the model surrogate organism *M. aurum* was also tested (Table 5).[27] Efflux pumps are transport proteins involved in the extrusion of toxic substrates, including virtually all classes of anti-mycobacterial drugs, from within cells into the external environment. Pumps may be specific for one substrate or may transport a range of structurally dissimilar compounds and can be associated with MDR in MTB. Thus, the identification of efflux pump inhibitors can lead to new anti-tubercular agents able to reverse drug resistance in TB and to be used in combination therapy together with first line drugs.

DISCUSSION

We first analysed the data arising from the screening on non-pathogenic *M. tuberculosis* mc^27000 (Table 4). In agreement with our initial hypothesis, the insertion of a 1- and a 2-adamantyl-piperazine group in place of the *N*-methylpiperazine of **1** led to **7l** and **7k** with significantly contrasting activity. In fact, **7k**, bearing the same 2-adamantyl group found in **2**, was inactive (MIC value > 64 μg/mL). On the contrary, the corresponding 1-adamantyl analogue **7l** showed a strong ability to inhibit MTB mc^27000 growth, with a MIC value of about 0.5 μg/mL. Compound **7l** was then chosen as the most representative compound to be further studied for deducing SAR considerations on the new class of hybrid compounds on MTB mc^27000. In particular, according to the suggestions derived from the superposition pattern between **1** and **2**, the *p*-Cl phenyl moiety at C5 of **7l** was simplified to a methyl group, leading to **7i** with a significant 16-fold drop in activity (8.0 μg/mL). The corresponding 2-adamantyl analogue **7a** showed a slight increase in activity (3.3 μg/mL). Moreover, small changes in substituents and substitution pattern at its 1-phenyl ring clearly showed that small substituents (isopropyl and fluorine) at para and ortho positions (such as in **7c** and **7b**) guaranteed activity retention or

enhancement (3.3 and 1.0 μg/mL, respectively). Differently, a *m*-methyl group as in **7d** caused a significant drop in activity (32 μg/mL), in agreement with that previously found for derivatives of **1**.[8] Decreasing the bulkiness of the hydrophobic moiety on the piperazine ring from an adamantyl (such as in **7i** or **7a**) to a norbornane group led to a slight improvement of activity (MIC of **7g** was 2.0 μg/mL). On the contrary, a further simplification to a cyclohexyl ring (**7h**) and its aromatization to a phenyl ring (**7e**) further reduced activity to 8.0 and 32 μg/mL, respectively. Introduction of a second *p*-Cl phenyl moiety at C5 of **7e** restored a 1.0 μg/mL activity in **7j**. SAR considerations on both **7j** and **7e** (1.0 and 32 μg/mL, respectively) suggested that in several cases the presence of the *p*-Cl phenyl moiety at C5 could improve anti-mycobacterial activity. On the other hand, a comparison between activity of **7e** and its adamantyl analogues **7i** and **7a** (8.0 and 3.3 μg/mL, respectively) clearly showed that the *p*-Cl phenyl moiety at C5 was not mandatory for obtaining active compounds, as suggested by the common feature model. Also the comparison of the biological profiles of the norbornyl derivatives **7g** and **7m** clearly shows that the *p*-Cl phenyl moiety at C5 in **7m** is detrimental for the anti-tubercular activity. Moreover, the comparable anti-mycobacterial activities of **7j** and **7l** (1.0 and 0.5 μg/mL, respectively) allowed us to hypothesize that the distal nitrogen atom of the piperazine ring (that is protonatable in **7l**, while has an anilino character in **7j**) could be unimportant for activity. This result was in agreement with previous pharmacophoric-based calculations and in vitro activity of piperidine analogues of **1**.[9] To validate this hypothesis, compounds with a linear amino spacer instead of the piperazine ring were synthesized. Among them, **9a** had an overall size comparable to that of **7e** and lacked the distal nitrogen atom of the parent piperazine ring. Its activity was 8-fold better than that of the piperazine analogue **7e** (4.0 and 32 μg/mL, respectively). Attempts to modify the phenylethylamino side chain of **9a** by introduction of an oxygen atom (as in **11a** and

11b) or by partial rigidification into an aryloxime (as in **10a**) led to inactive compounds (>64 μg/mL). Alternatively, shortening the phenylethylamino spacer led to very active compounds. As an example, the benzylamino analogue **9b** showed a 0.5 μg/mL MIC value. Decoration of the para position of the terminal phenyl ring with small substituents (such as a F, Cl, and Me) led to **9g**, **9f**, and **9e** with comparable or slightly lower activity (0.7, 2.0, and 2.0 μg/mL, respectively), further confirming that the distal nitrogen atom of the piperazine ring was not necessarily required for anti-mycobacterial activity of the new hybrid compounds. On the contrary, replacement of the *p*-Cl of **9b** with a *p*-F group as in **9h** caused an 8-fold drop in activity (from 0.5 to 4.0 μg/mL). A further reduction of the amino side chain length to a cyclohexylamino and to the bulky 2-adamantylamino moiety as in **9c** and **9d**, respectively, also maintained a 0.5 and 1.0 μg/mL activity. Interestingly, when the methyl group at C5 of compounds **9b** and **9c** was replaced with a *p*-Cl phenyl moiety leading to derivatives **9i** and **9j**, a significant drop in activity was observed (16 and 8 μg/mL respectively). Compounds **9b-c** proved to be much more active than **1** against MTB $mc^2$7000. These latter data confirm the initial hypothesis that an aryl substituent at C5, such in **1**, is not mandatory to obtain derivatives active against *M. tuberculosis*. Also the new compounds bearing a secondary amine show a better activity profile than **2**, thus pointing out that a diamine backbone could be not essential for antitubercular activity.

The same compounds were also assayed on additional mycobacterial strains. Activity against the pathogenic MTB H37Rv (Table 4) followed the same trend already shown for the MTB $mc^2$7000 strain. The only exceptions were represented by **9f** and **9g** that were inactive or weakly active toward MTB H37Rv (16 and >125 μg/mL, respectively), while their congener compounds **9e** and **9b** showed a 1.0 and 0.5 μg/mL activity. The hybrid compounds **7a-b**, **7e** and **7h** showed

a good profile with MIC = 7.8 and 3.9 μg/mL. The derivative **7j** bearing a *p*-Cl-phenyl substituent at C5 showed an improved biological profile (1.9 μg/mL). On the other hand, the simplified compounds **9** showed higher activity against MTB H37Rv than derivatives **7**. In particular, compounds **9b** and **9c** proved to be very active showing again activity (0.5 and 0.2 μg/mL respectively) comparable or better than **1** and **2**.

Moreover, as a general trend, the hybrid compounds showed weak activity toward *M. smegmatis* mc^2155 (MIC values ranging from 4.0 to >64 μg/mL, with only two compounds showing better activity – 3.3 and 2.0 μg/mL, respectively). Table 3. Similarly, *M. aurum* was scarcely sensitive to the test compounds: only four compounds (namely, **9b**, **9e**, **9f**, and **9g**) showed a MIC value of about 2.0 μg/mL (Table 3). As the whole genome sequence of *M. aurum* has been published recently, comparative genomic analyses of these transporter proteins should elucidate why the difference in their drug susceptibilities is observed.[25] In general, fast growing mycobacteria (*M. aurum* and *M. smegmatis*) were inhibited at higher concentration than other strains. A better anti-mycobacterial activity profile was found toward *M. bovis* BCG (Table 3), with ten compounds showing activity value in the range below 4.0 μg/mL and three compounds (namely, **9b**, **9c**, and **9g)** with a MIC value of 0.5 μg/mL. Among MDR-TB strains (Table 4), MDR2 was poorly sensitive to the test compounds, with the only exception of **9a** and **9b** which showed a good activity at 7.8 μg/mL and 3.9 μg/mL. On the other hand, MDR1 growth was blocked by at least 7 compounds with MIC values lower than 4.0 μg/mL. Of particular interest were compounds **9b** and **9c** that showed MIC values of about 1.0 and 0.5 μg/mL, respectively, much better than that of the parent compound **1** and isoniazid.

An analysis of anti-mycobacterial data clearly showed that the best compounds (**9a**, **9b**, and **9c**) were characterized by structural features significantly different from those of the parent compound **1**. In particular, they lacked both the second aryl moiety at the position C5 of the pyrrole nucleus and the distal nitrogen atom of the original piperazine ring. Moreover, the overall activity underwent an improvement when the basic linear side chain was shortened from the phenylethylamino of **9a**, to the benzylamino of **9b**, to the cyclohexylamino of **9c**.

The C5 aryl moiety was not a mandatory substituent for active compounds, and small groups are allowed as decoration of the N1-phenyl ring. A bulky terminal group, such as an adamantane and a norbornane, improve the activity of piperazine analogues, while a significant gain of anti-mycobacterial activity resulted from piperazine replacement by linear aryl and alkylamino side chains.

The high anti-mycobacterial activity maintained even after a significant structural simplification of 1,5-diarylpyrroles (derivatives and analogues of **1**) into the corresponding 1-aryl hybrid analogues could be accounted by a comparison of the original pharmacophoric model for anti-mycobacterial compounds belonging to the pyrrole class of **1**[8] with the simplified common feature model described here. In fact, the original pharmacophoric model[8] was able to accommodate **1** and its derivatives in two different orientations, rotated of about 180 degrees around the pyrrole plane. Following this, the aryl moieties at positions N1 and C5 of **1** could reciprocally change their spatial location and, consequently, match with the pharmacophore. These results suggested that the pharmacophoric portions able to accommodate the substituents at positions N1 and C5 are redundant and could be simplified, as also suggested by the superposition between **1** and **2**.

In a further attempt to codify the structural features of the new hybrid pyrroles, a second generation common feature model was built starting from a larger set of compounds, comprised of **1**, **2**, and the most active pyrroles (with MIC values ≤ 1.0 μg/mL). The improved model (Figure 3) showed that the distal nitrogen of the piperazine ring of **1** (corresponding to P8 in the previous common feature model) was omitted, while an additional hydrophobic region (H2), adjacent to the P7 feature (a positively ionizable feature), accommodated the terminal hydrophobic groups of the C3 side chain.

In order to prove the effectiveness of our compounds, the cytotoxicity of the novel pyrroles was then evaluated on RAW264.7 cells as well as THP-1 cell lines. Compounds **7j**, **9c** and **9h** showed an excellent cytotoxicity profile, with a selectivity index (SI) of 92, 50 and 5.6 against RAW264.7 and 155, 37 and 28 against THP-1 cells respectively. Both **7j** and **9c** showed a better cytotoxicity profile than **1** against the murine and human cells (Table 4).

Finally, the effect of pyrroles on the efflux pump inhibitory (EPI) activity of the model surrogate organism *M. aurum* was tested in order to identify compounds able to reverse multi-drug resistance in TB (Table 5, Figure 4). An efflux pump activity whole cell-based assay has been carried out and, as a consequence, the results account for the total activity of the whole population of efflux pumps present in the cells. The efflux pump assay revealed that most of pyrrole compounds (barring **7k**) possess at least low to moderate inhibitory property. However, a weak correlation between inhibition of bacterial growth and efflux pump mechanism is observed. For example, **9a-c** are very efficient in killing mycobacterial cells but only display moderate modulatory effect on the pumps. On the other hand, **11b** inhibits efflux inhibition at par with the control inhibitor Verapamil, but shows almost no effect on the growth of these cells. Interestingly, **7c**, **7h**, **7i**, and **7l**, bearing a bulky alkyl substituent on the piperazine ring, showed

good/excellent inhibitory activity. These findings confer that specific endogenous targets for these compounds are still elusive, however indicate that they may have a pleiotropic modes of action and potential to reverse anti-microbial resistance. As TB treatment regimens always comprise of a combination of complimentary drugs, this off-target effect of the compounds could have a positive impact on the effectiveness of drug treatment regimens. Within this context it is noteworthy that five compounds (**11b**, **7c**, **7h**, **7i**, **7l**) show a much higher efflux pump inhibitory activity than **1** and **2** (Table 5), who are known inhibitors solely of the pump transporter MmpL3. In fact, the less potent mycobacterial growth inhibitors showing higher whole-cell efflux inhibitory properties may also prove prospective leads in a multi-drug therapy owing to synergistic combinations should that arise. Thus, unlike **1** and **2** which show poor EPI activity, **11b** and **7b** could be used in combination with standard antitubercular drugs such isoniazid or rifampin to reverse multi-drug resistance in tuberculosis.

CONCLUSIONS

In conclusion, a library of pyrrole derivatives was successfully synthesized and evaluated for their anti-tubercular activity against MTB and MDR-TB clinical isolates. The new pyrroles were designed as hybrids of the anti-mycobacterial agents **1** and **2**. Five compounds showed anti-tubercular activity on MTB at ≤1.0 μg/mL, and two of them (**9b** and **9c**) proved to be highly active also against MDR-1 TB strains. SAR studies revealed the key features essential for the anti-mycobacterial activity. Finally, the potent anti-tubercular derivative **9c** showed low eukaryotic cell toxicity, turning out to be an excellent lead candidate for preclinical trials. In general, compound **9c** showed a better drug profile than **1** in terms of activity, cytotoxicity and potency toward MDR-TB clinical isolates. The pharmacokinetics parameters of **9b** and **9c** will

be evaluated in due course and compared with those of **1** in order to prove the efficacy of the new compounds and to progress toward preclinical trials.

EXPERIMENTAL SECTION

Computational details

The structures of all the molecules were sketched using Maestro[28] and then subjected to LigPrep program to generate high-quality, all-atom 3D structures to be used as the input for next calculations. The OPLS_2005 force field was applied, and possible ionization states were generated for the structures at pH 7±2 using Epik.

Conformers were generated by MacroModel[29] with the Systematic Pseudo Monte Carlo (a systematic torsional sampling protocol) search algorithm, OPLS-2005 force field with implicit GB/SA distance-dependent dielectric solvent model (water as the solvent) at cutoff root mean square deviation of 0.5 with 1000 steps. All the conformers were subsequently minimized using Polak-Ribiere Conjugate Gradient minimization with 5000 iteractions. For each molecule, a conformer set with a maximum energy difference of 25 kcal/mol relative to the global energy minimum conformer was stored.

Both **1** and **2** were used to build three-dimensional common feature models comprised of chemical features common to the two compounds. Considering the reduced number of compounds and the fact that their anti-mycobacterial activity was assayed by different research groups with different tests, we chose to apply a common feature hypothesis generation routine, instead of building a quantitative model. Phase[20] software has been applied to generate the models. Minimum and maximum number of sites for all the features were set to 4 and 5,

respectively. Only the positively ionizable group (P) and the hydrophobic region (H) features were used to build a series of hypotheses, while the aromatic ring (R) feature was not further considered by the software because it was not present in the structure of **2**. The resulting four-feature hypotheses were constituted by two H and two P features.

Biology experimental part

Bacterial strains and growth conditions: The bacterial species used in this study were *M. smegmatis* mc^{2}155 (ATCC 700084), *M. aurum* (ATCC23366), *M. bovis* BCG Pasteur (ATCC 35734), *M. tuberculosis* mc^{2}7000,[30-32] *M. tuberculosis* H37Rv (ATTC27294), and two MDR-TB clinical isolates (MDR1 and MDR2) obtained from Royal Free Hospital NHS Trust, London, UK. The cell line utilised for cytotoxicity studies were the murine macrophage cell line RAW264.7 (ATCC TIB-71) and the human peripheral blood monocyte-derived cell line THP-1. Mycobacterial species were cultured in either Middlebrook 7H9 broth or Middlebrook 7H10 agar media supplemented with albumin-dextrose-catalase (ADC) or oleic acid-albumin-dextrose-catalase (OADC) enrichments, respectively, purchased from BD Biosciences. All reagents were purchased from Sigma-Aldrich unless stated otherwise.

Bacterial growth inhibition assays.

Anti-mycobacterial activity: HT-SPOTi was used as described previously[33-35] to assess the minimum inhibitory concentrations of the compounds on *M. aurum*,[27] *M. tuberculosis* H37Rv, and the MDR strains of the pathogen. Briefly, the assay was conducted in a semi-automated 96 well plate format. The compounds were dissolved in a suitable solvent to a concentration of 50 mg/mL and serially diluted (two-fold dilutions). 2 μL of each dilution were dispensed into a well of a 96-well plate to which 200 μL of Middlebrook 7H10 agar medium kept at 55 °C

supplemented with 0.05% (*v/v*) glycerol and 10% (*v/v*) OADC was added. The concentration ranges of the compounds used was 500-0.5 μg/mL. A well with no compounds (DMSO only) and isoniazid was used as experimental control. To all the plates, a drop (2 μL) of early to mid-log bacterial culture containing $2x10^3$ colony forming units (CFUs) was spotted in the middle of each well and the plates were incubated at 35 or 37 °C depending on the bacterial species and incubated till distinct spots were observed in the control wells (this took 4 days in the case of *M. aurum* and 7 days in the case of *M. tuberculosis* H37Rv and 9 days for its drug resistant clinical isolates). The MICs were determined as the lowest concentration of the compound where mycobacterial growth was completely inhibited.

The MIC of the compounds against *M. smegmatis* mc^2155, *M. bovis* BCG, and *M. tuberculosis* mc^27000 were calculated by standard MABA (Microplate Alamar Blue assay) as previously described.[30] Briefly, 200 μL of sterile deionized water was added to all outer-perimeter wells of a sterile 96-well plate (Corning Incorporated, Corning, NY) to minimize evaporation of the medium in the test wells during incubation. The wells in rows B to G in columns 3 to 11 received 100 μL of 7H9 medium containing 0.2% casamino acids, 24 μg/mL pantothenate and 10% OADC (Beckton Dickinson, Sparks, MD). Compounds were added to rows B–G followed by 1:2 serial dilutions across the plate to column 10, and 100 μL of excess medium was discarded from the wells in column 10. The bacterial culture at 0.5 McFarland standard diluted 1:25 (100 μL) was added to the wells in rows B to G in columns 2 to 11, where the wells in column 11 served as drug-free controls. The plates were sealed with parafilm and were incubated at 37 °C. A freshly prepared 1:1 mixture of Alamar Blue (Celltiter-Blue™, Promega Corp, Madison, WI) reagent and 10% Tween® 80 (50 μL) and re-incubated at 37 °C for 24 h.

Eukaryotic cell toxicity and selectivity indices: The cell lines were grown and maintained in RPMI-1640 supplemented with 10% FBS incubated at 37°C with 5% CO_2 in a humidified incubator. For the experiment, 2 µL of the 50 mg/mL stock solution of each compound was diluted in 200 µL of RPMI-1640 medium in the first row of a 96-well microplate and two fold dilutions were performed along the rows leaving the last one (Row- H) as a solvent control. 100 µL containing 10^5 cells/mL of confluent murine macrophage cells (RAW 264.7) or THP-1 cells in logarithmic growth phase were added to each well. The plates were incubated at 37 °C in a humidified CO_2 incubator (5% CO_2) for 48 h. Each well was washed twice with 1x PBS, and 170 µL fresh RPMI-1640 was added to each well followed by 30 µL of 0.01% trypan blue. AS THP-1 cells are suspension cultures, the plates were centrifuged between the washing steps. After overnight incubation, the change in colour was observed and the fluorescence intensity was measured at $\lambda_{exc}560/\lambda_{emi}590$ nm.

Assaying whole-cell drug efflux pump inhibition: The assay was modified from previously published protocol.[36] Early log phase cells of *M. aurum* (OD_{600} ~ 0.8) were taken and the OD_{600} was adjusted to 0.4 by diluting the cells with culture medium. The cells were collected by centrifugation and resuspended in equivalent volume 1x PBS. The test samples contained: 4-6x10^7 bacteria/mL in PBS, 0.4% glucose (as a source of energy for efflux pumps activity), 0.5 mg/L ethidium bromide (as a substrate for efflux pumps) and the compounds being tested at 1/4x-MIC concentrations. Blank samples contained all of the components mentioned above except the bacterial suspension, which was replaced with 1x PBS. Verapamil, a known efflux pump inhibitor was used as the positive control at a concentration of 125 µg/mL. Compounds **1** and **2** were also included in the experiment to obtain a comparison between them and the newly synthesised compounds with regards to their efflux inhibitory properties. The experiment was

performed in a 96-well plate which was placed in a fluorimeter (FLUOstar OPTIMA, BMG Labtech, UK) and the instrument was programmed with the following parameters: wavelengths of 544 nm and 590 nm for excitation and detection of fluorescence, gain 2200, a temperature of 37 °C, and a cycle of measurement every minute for a total period of 60 min. The accumulation or efflux of ethidium bromide was monitored for the mentioned period on a real-time basis.

Chemistry - Materials and methods

^{1}H NMR and ^{13}C NMR spectra were recorded on JEOL Delta-270 or JEOL ECS-400 spectrometers operating at the frequencies indicated. Chemical shifts (δ) are in ppm, referenced to tetramethylsilane. Coupling constants (J) are reported in Hertz and rounded to 0.5 Hz. Splitting patterns are abbreviated as follows: singlet (s), doublet (d), triplet (t), quartet (q), multiplet (m), broad (br) or some combination of them. Infrared spectra were obtained using a Durascope diamond ATR system. Mass spectra (HRMS) were recorded at the EPSRC National Mass Spectrometry Service Centre on a Thermo Scientific LTQ Orbitrap XL Mass Spectrometer using low-resolution ESI or high-resolution nanoESI techniques. The purity of the compounds was assessed by reverse-phase liquid chromatography coupled with a mass spectrometer (Agilent series 1100 LC/MSD) with a UV detector at k = 254 nm and an electrospray ionization source (ESI). HPLC analyses were performed at 0.4 mL/min flow rate and using a binary solvent system of 95:5 methyl alcohol/water. All the solvents were of HPLC grade. Mass spectra were acquired in positive mode scanning over the mass range of 50–1500. The following ion source parameters were used: drying gas flow, 9 mL/min; nebulize pressure, 40 psig; and drying gas temperature, 350 ºC. All target compounds possessed a purity of ≥ 95% as verified by HPLC analyses. TLC was performed using commercially available pre-coated plates and visualized with UV light at 254 nm; K_2MnO_4 was used to reveal the products. Flash column

chromatography was carried out using Fluorochem Davisil 40-63 u 60 Å. All reactions were conducted under a nitrogen atmosphere in oven-dried glassware unless stated otherwise. THF was distilled under nitrogen from sodium using a benzophenone indicator. Dichloromethane was purchased from Aldrich. Acetonitrile was further dried over 4 Å oven-activated molecular sieves for 1 h prior to use. Petrol refers to the fraction of light petroleum ether boiling between 40 and 65 °C. All other solvents and commercially available reagents were used as received.

Pyrroles **3a-e** were synthesised as described in the literature.[18]

Synthesis of alkyl piperazines 6a-b. General procedure.

The Boc piperazine **4** (2 mmol) and the appropriate ketone **5** (2 mmol) were dissolved in THF (8 mL) and the resulting mixture was stirred for 5 minutes. The reaction was cooled at 0 °C and then $Na(AcO)_3BH$ (2.4 mmol) and AcOH (2 mmol) were carefully added. The resulting mixture was stirred at rt for 16 h. The reaction was quenched with NaOH 1N (20 mL) and the product was extracted with AcOEt (3 x 25 mL). The AcOEt extract was dried ($MgSO_4$), and the solvent was evaporated to give the crude piperazine derivatives which were filtered through a pad of silica gel (eluent AcOEt/petroleum ether 1:1). The filtered compounds were then dissolved in DCM (4 mL) and treated with 1 mL TFA. The resulting mixture was stirred at rt for 12 h. The solvents were removed and the crude compound was dissolved in AcOEt (10 mL) and washed several times with 1N NaOH (20 mL). The organic phase was dried ($MgSO_4$), and the solvent was evaporated to yield the crude piperazines **6a-b** which were purified by column chromatography using petroleum ether/AcOEt 1:1 as eluent.

1-(Adamantan-2-yl)piperazine (6a). Tan oil. ^{1}H NMR (400 MHz $CDCl_3$) δ 3.31 (m, 4H), 2.81 (m, 2H), 2.31 (br s, 2H), 2.01-1.94 (m, 4H), 1.76-1.68 (m, 5H), 1.60-1.53 (m, 4H), 1.42-1.39 (m, 1H), 1.30-1.27 (m, 1H) ppm. LRMS m/z (ES+) m/z: 221 $[M+H]^+$

1-(Bicyclo[2.2.1]heptan-2-yl)piperazine (6b). Tan oil. ^{1}H NMR (400 MHz $CDCl_3$) δ 2.88-2.82 (m, 5H), 2.28 (br s, 3H), 2.20-2.09 (m, 3H), 1.67-1.60 (m, 2H), 1.41-1.39 (m, 1H), 1.28-1.19 (m, 4H), 0.82-0.79 (m, 1H) ppm. LRMS m/z (ES+) m/z: 181 $[M+H]^+$

Synthesis of pyrrole derivatives 7a-m. General Procedure.

Following the Mannich reaction, to a stirred solution of an appropriate pyrrole **3a-e** (1.5 mmol) in acetonitrile (5 mL), a mixture of the appropriate piperazine **6** (1.5 mmol), formaldehyde (1.5 mmol) (40% in water), and 1.3 mL of acetic acid was added dropwise. After the addition was complete, the mixture was stirred at rt for 3 h. The mixture was then treated with a solution of sodium hydroxide (20%, w/v) (20 mL) and extracted with AcOEt (10 mL). The organic extracts were combined, washed with water, and dried. After removal of solvent, the residue was purified by column chromatography, using silica gel and petroleum ether/ethyl acetate (4:1 v/v) as eluent.

1-(Adamantan-2-yl)-4-((1-(4-chlorophenyl)-2,5-dimethyl-1H-pyrrol-3-yl)methyl)piperazine (7a). R_f 0.11 (AcOEt/hexane 1:1). Tan oil. ^{1}H NMR (400 MHz $CDCl_3$) δ 7.41 (d, 2H, J = 8.7 Hz), 7.12 (d, 2H, J = 8.7 Hz), 5.92 (s, 1H), 3.36 (s, 2H), 2.50 (br s, 4H), 2.05-2.02 (m, 6H), 1.98 (s, 3H), 1.95 (s, 3H), 1.85-1.72 (m, 5H), 1.68-1.62 (m, 5H), 1.37-1.34 (m, 3H) ppm. ^{13}C NMR (100 MHz $CDCl_3$) δ 137.7, 133.4, 129.7, 129.3, 127.6, 126.8, 115.2, 108.7, 67.9, 54.4, 53.5, 49.6, 37.9, 37.3, 31.6, 31.4, 29.0, 27.6, 27.4, 22.7, 14.2, 12.9, 11.0 ppm. LRMS m/z (ES+) m/z: 439 $[M+1]^+$. HRMS (ESI): calcd for $C_{27}H_{37}ClN_3$ ($M + H^+$) 438.2671, found 438.2664.

1-(Adamantan-2-yl)-4-((1-(2-fluorophenyl)-2,5-dimethyl-1H-pyrrol-3-yl)methyl)piperazine (7b). R_f 0.15 (AcOEt/hexane 1:1). Tan oil. ^{1}H NMR (400 MHz $CDCl_3$) δ 7.37-7.36 (m, 1H), 7.22-7.17 (m, 3H), 5.95 (s, 1H), 3.36 (s, 2H), 2.59-2.29 (br s, 4H), 2.08-2.03 (m, 6H), 1.97 (s, 3H), 1.93 (s, 3H), 1.83-1.75 (m, 5H), 1.67-1.62 (m, 5H), 1.36-1.24 (m, 3H) ppm. ^{13}C NMR (100 MHz $CDCl_3$) δ159.81, 157.31, 130.84, 129.6, 128.06, 127.2, 126.9, 124.5, 124.4, 116.7, 116.5, 115.3, 108.6, 67.9, 54.6, 53.6, 49.6, 47.0, 39.3, 37.3, 36.3, 31.9, 31.4, 29.04, 27.6, 27.5, 22.7, 14.2, 12.4, 10.5 ppm. LRMS m/z (ES+) m/z: 422 $[M+1]^+$. HRMS (ESI): calcd for $C_{27}H_{37}FN_3$ ($M + H^+$) 422.2966, found 422.2889.

1-(Adamantan-2-yl)-4-((1-(4-isopropylphenyl)-2,5-dimethyl-1H-pyrrol-3-yl)methyl)piperazine (7c). R_f 0.2 (AcOEt/hexane 1:1). Tan oil. ^{1}H NMR (400MHz $CDCl_3$) δ 7.27-7.24 (m, 2H), 7.10-7.04 (m, 2H), 5.91 (s, 1H), 3.46 (s, 2H), 2.97-2.92 (m, 1H), 2.52 (br s, 4H), 2.06-2.03 (m, 6H), 1.95 (s, 3H), 1.93 (s, 3H), 1.83-1.75 (m, 5H), 1.68-1.62 (m, 5H), 1.29 (s, 3H), 1.27 (s, 3H), 1.25 (m, 3H) ppm. ^{13}C NMR (100MHz $CDCl_3$) 148.2, 136.6, 128.2, 128.1, 127.9, 127.1, 126.9, 108.0, 67.9, 54.5, 53.4, 50.8, 49.5, 37.9, 37.3, 33.8, 31.6, 31.4, 29.0, 27.6, 27.4, 24.0, 22.7, 14.2, 12.9, 11.2, 11.0 ppm. LRMS m/z (ES+) m/z: 446 $[M+H]^+$. HRMS (ESI): calcd for $C_{30}H_{44}N_3$ ($M + H^+$) 446.3530, found 446.3523.

1-(Adamantan-2-yl)-4-((1-(3-methylphenyl)-2,5-dimethyl-1H-pyrrol-3-yl)methyl)piperazine (7d). R_f 0.17 (AcOEt/hexane 1:1). Tan oil. ^{1}H NMR (400MHz $CDCl_3$) δ 7.32-7.29 (m, 1H), 7.18-7.16 (m, 1H), 6.99-6.95 (m, 2H), 5.91 (s, 1H), 3.39 (s, 2H), 2.53 (br s, 4H), 2.38 (s, 3H), 2.03 (m, 6H), 1.99 (s, 3H), 1.95 (s, 3H), 1.83-1.75 (m, 5H), 1.68-1.62 (m, 5H), 1.37-1.34 (m, 3H) ppm. ^{13}C NMR (100MHz $CDCl_3$) δ 139.1, 138.9, 129.0, 128.7, 128.3, 127.7, 125.4, 108.2, 67.9, 54.5, 53.4, 49.5, 41.0, 37.9, 37.3, 31.4, 29.03, 28.5, 27.6, 27.4, 21.3, 12.9,

11.0 ppm. LRMS m/z (ES+) m/z: 418 $[M+1]^+$. HRMS (ESI): calcd for $C_{28}H_{40}N_3$ ($M + H^+$) 418.3217, found 418.3234.

1-((1-(4-Chlorophenyl)-2,5-dimethyl-1H-pyrrol-3-yl)methyl)-4-phenylpiperazine (7e). Tan oil. R_f 0.43 (AcOEt/hexane 1:1). ^{1}H NMR (400 MHz $CDCl_3$) δ 7.44 (d, 2H, J = 8 Hz), 7.26 (dd, 2H, J = 8.7, 7.3 Hz), 7.15 (d, 2H, J = 7 Hz), 6.94 (d, 2H, J = 7 Hz), 6.85 (m, 1H), 5.96 (s, 1H), 3.45 (s, 2H), 3.23 (m, 4H), 2.66 (m, 4H), 2.02 (s, 3H), 2.00 (s, 3H) ppm. ^{13}C NMR (100 MHz $CDCl_3$) δ 151.5, 137.6, 133.5, 129.7, 129.3, 129.1, 127.8, 126.8, 119.5, 115.0, 108.6, 54.5, 52.9, 49.2, 12.9, 11.0 ppm. LRMS m/z (ES+) m/z: 380 $[M+1]^+$. HRMS (ESI): calcd for $C_{23}H_{27}ClN_3$ ($M + H^+$) 380.1888, found 380.1884.

4,4'-((1-(4-Chlorophenyl)-2,5-dimethyl-1H-pyrrole-3,4-diyl)bis(methylene))bis(1-phenylpiperazine) (7f). Tan oil. R_f 0.25 (AcOEt/hexane 1:1). ^{1}H NMR (400 MHz $CDCl_3$) δ 7.30-7.28 (d, 2H, J = 8.2 Hz), 7.08 (dd, 4H, J = 8.5, 7.6 Hz), 7.01 (d, 2H, J = 8.7 Hz), 6.77 (d, 4H, J = 8.2 Hz), 6.66 (m, 2H), 3.34 (s, 4H), 3.03 (m, 8H), 2.47 (m, 8H), 1.85 (s, 6H) ppm. ^{13}C NMR (100 MHz $CDCl_3$) δ 151.5, 137.7, 133.4, 129.8, 129.3, 129.1, 126.5, 119.5, 116.0, 53.0, 52.8, 11.0 ppm. LRMS m/z (ES+) m/z: 555 $[M+1]^+$. HRMS (ESI): calcd for $C_{34}H_{41}ClN_5$ ($M + H^+$) 554.3045, found 554.3032.

1-((1S,4R)-Bicyclo[2.2.1]heptan-2-yl)-4-((1-(4-chlorophenyl)-2,5-dimethyl-1H-pyrrol-3-yl)methyl)piperazine (7g). R_f 0.15 (AcOEt/hexane 1:1). Tan oil. ^{1}H NMR (400 MHz $CDCl_3$) δ 7.40 (d, 2H, J = 5 Hz), 7.11 (d, 2H, J = 5 Hz), 5.90 (s, 1H), 3.37 (s, 2H), 2.48 (br m, 5H), 2.24-2.12 (m, 4H), 1.97 (s, 3H), 1.94 (s, 3H), 1.72-1.65 (m, 2H), 1.46 (m, 1H), 1.33-1.22 (m, 5H), 0.88-0.81 (m, 2H) ppm. ^{13}C NMR (100 MHz $CDCl_3$) δ 137.7, 133.4, 129.7, 129.3, 127.6, 126.8, 115.2, 108.7, 67.9, 54.4, 52.8, 52.7, 39.0, 38.1, 36.8, 35.8, 30.6, 21.1, 12.8, 11.0 ppm. LRMS

m/z (ES+) m/z: 398 $[M+H]^+$. HRMS (ESI): calcd for $C_{24}H_{33}ClN_3$ ($M + H^+$) 398.2358, found 398.2352.

1-((1-(4-Chlorophenyl)-2,5-dimethyl-1H-pyrrol-3-yl)methyl)-4-cyclohexylpiperazine (7h). Tan oil. R_f 0.15 (AcOEt/hexane 1:1). ^{1}H NMR (400 MHz $CDCl_3$) δ 7.40 (d, 2H, J = 5 Hz), 7.10 (d, 2H, J = 5 Hz), 5.89 (s, 1H), 3.37 (s, 2H), 2.60 (br s, 8H), 2.20 (m, 1H), 1.96 (s, 3H), 1.93 (s, 3H), 1.88-1.86 (m, 2H), 1.77-1.75 (m, 2H), 1.61-1.58 (m, 1H), 1.26-1.11 (m, 5H) ppm. ^{13}C NMR (100 MHz $CDCl_3$) δ 137.6, 133.5, 129.7, 129.6, 129.3, 127.7, 118.7, 108.7, 63.5, 56.2, 54.3, 53.0, 48.8, 29.0, 26.3, 25.9, 12.8, 11.0, 10.5 ppm. LRMS m/z (ES+) m/z: 386 $[M+H]^+$. HRMS (ESI): calcd for $C_{23}H_{33}ClN_3$ ($M + H^+$) 386.2358, found 386.2356.

1-(Adamantan-1-yl)-4-((1-(4-chlorophenyl)-2,5-dimethyl-1H-pyrrol-3-yl)methyl)piperazine (7i). R_f 0.10 (AcOEt/hexane 1:1). Tan oil. ^{1}H NMR (400 MHz $CDCl_3$) δ 7.41 (d, 2H, J = 8.7 Hz), 7.10 (d, 2H, J = 8.7 Hz), 5.89 (s, 1H), 3.38 (s, 2H), 2.67 (br s, 4H), 2.50 (br s, 4H), 2.05 (m, 4H), 1.96 (s, 3H), 1.93 (s, 3H), 1.69-1.59 (m, 11H) ppm. ^{13}C NMR (100 MHz $CDCl_3$) δ 137.7, 133.4, 129.7, 129.8, 129.3, 127.6, 126.8, 115.0, 108.8, 60.4, 56.1, 54.2, 53.5, 44.0, 38.5, 37.0, 31.6, 29.7, 25.3, 22.7, 20.7, 18.8, 14.1, 11.0 ppm. LRMS m/z (ES+) m/z: 439 $[M+H]^+$. HRMS (ESI): calcd for $C_{27}H_{37}ClN_3$ ($M + H^+$) 438.2671, found 438.2680.

1-((1,5-Bis(4-chlorophenyl)-2-methyl-1H-pyrrol-3-yl)methyl)-4-phenylpiperazine (7j). White solid, mp 169 ºC. R_f 0.2 (AcOEt 100%). ^{1}H NMR (400 MHz $CDCl_3$) δ 7.33 (d, 2H, J = 8.2 Hz), 7.23 (m, 2H), 7.07 (dd, 4H, J = 16.9, 8.2 Hz), 6.92 (m, 4H), 6.82 (m, 1H), 6.36 (s, 1H), 3.49 (s, 2H), 3.21 (m, 4H), 2.67 (m, 4H), 2.07 (s, 3H) ppm. ^{13}C NMR (100 MHz $CDCl_3$) δ 151.4, 137.8, 133.5, 132.0, 131.7, 131.5, 130.3, 129.8, 129.4, 129.1, 128.8, 128.4, 119.7, 116.9, 116.1,

111.7, 54.5, 52.9, 49.2, 11.3 ppm. LRMS m/z (ES+) m/z: 477 $[M+H]^+$. HRMS (ESI): calcd for $C_{28}H_{28}Cl_2N_3$ ($M + H^+$) 476.1655, found 476.1648.

1-(Adamantan-2-yl)-4-((1,5-bis(4-chlorophenyl)-2-methyl-1H-pyrrol-3-yl)methyl)piperazine (7k). Yellow solid, mp 197 ºC. R_f 0.35 (AcOEt/MeOH 4:1). ^{1}H NMR (400 MHz $CDCl_3$) δ 7.34-7.32 (d, 2H, J = 4 Hz), 7.10-7.04 (m, 4H), 6.93 (d, 2H, J = 4 Hz), 6.36 (s, 1H), 3.44 (s, 2H), 2.54 (br s, 4H), 2.05 (s, 3H), 2.03 (m, 4H), 1.84-1.75 (m, 4H), 1.68-1.63 (m, 4H), 1.38-1.25 (m, 5H), 0.88-0.82 (m, 2H) ppm. ^{13}C NMR (100 MHz $CDCl_3$) δ 137.8, 133.4, 131.9, 131.5, 130.2, 129.8, 129.4, 128.8, 128.3, 117.1, 111.5, 67.9, 54.4, 53.5, 49.6, 37.9, 37.3, 31.6, 31.4, 29.0, 27.6, 27.4, 22.7, 14.2, 11.2 ppm. LRMS m/z (ES+) m/z: 534 $[M+H]^+$. HRMS (ESI): calcd for $C_{32}H_{38}Cl_2N_3$ ($M + H^+$) 534.2437, found 534.2425.

1-(Adamantan-1-yl)-4-((1,5-bis(4-chlorophenyl)-2-methyl-1H-pyrrol-3-yl)methyl)piperazine (7l). Yellow solid, mp 148 ºC. R_f 0.34 (AcOEt/MeOH 4:1). ^{1}H NMR (400 MHz $CDCl_3$) δ 7.34-7.32 (m, 2H), 7.10-7.03 (m, 4H), 5.92 (s, 1H), 6.91 (m, 2H), 6.33 (s, 1H), 3.48 (s, 2H), 2.72-2.70 (br d, 8H), 2.07-2.02 (m, 4H), 2.04 (s, 3H), 1.71-1.56 (m, 11H) ppm. ^{13}C NMR (100 MHz $CDCl_3$) δ 137.8, 133.4, 131.6, 131.5, 130.3, 129.7, 129.4, 128.8, 128.3, 125.1, 116.5, 111.9, 66.6, 54.1, 53.2, 44.0, 38.3, 36.9, 32.2, 29.7, 26.4, 23.5, 18.7, 13.2, 11.3 ppm. LRMS m/z (ES+) m/z: 535 $[M+H]^+$. HRMS (ESI): calcd for $C_{32}H_{38}Cl_2N_3$ ($M + H^+$) 534.2437, found 534.2424.

1-(Bicyclo[2.2.1]heptan-2-yl)-4-((1,5-bis(4-chlorophenyl)-2-methyl-1H-pyrrol-3-yl)methyl)piperazine (7m). Pale yellow solid, mp 81 ºC. R_f 0.40 (AcOEt/MeOH 4:1). ^{1}H NMR (400 MHz $CDCl_3$) δ 7.26 (d, 2H, J = 12 Hz), 7.04 (d, 2H, J = 12 Hz), 6.99 (d, 2H, J = 12 Hz), 6.85 (d, 2H, J = 12 Hz), 6.30 (s, 1H), 3.44 (s, 2H), 2.51 (brs, 6H), 2.19-2.17 (m, 2H), 2.12-2.07

(m, 1H), 2.00 (s, 3H), 1.66-1.62 (m, 2H), 1.43-1.40 (m, 1H), 1.29-1.17 (m, 7H) ppm. ^{13}C NMR (100 MHz $CDCl_3$) δ 137.8, 133.4, 131.9,131.5, 129.7, 128.7, 128.3, 111.8, 67.9, 65.9, 54.2, 52.6, 38.9, 38.0, 36.8, 36.8, 31.6, 30.6, 22.7, 21.0, 14.2, 11.2 ppm. LRMS m/z (ES+) m/z: 494 $[M+H]^+$. HRMS (ESI): calcd for $C_{29}H_{34}Cl_2N_3$ ($M + H^+$) 494.2124, found 494.2113.

Synthesis of compounds 8a-c. General procedure.

$POCl_3$ (6 mmol) was added dropwise to a round bottom flask containing ice-cooled DMF (5 mL) under N_2 atmosphere. After 15 min, a solution of the appropriate pyrrole **3a-b** and **3e** (1 mmol) was added to the stirring solution. Then the reaction mixture was allowed to stir at 100 ºC for 3 h. The reaction was monitored through TLC. After completion, the reaction was quenched with 10% w/v NaOH solution (20 mL). The reaction mixture was then diluted with EtOAc (10 mL), washed two times with EtOAc (10 mL) and once with brine (20 mL). The organic extracts were collected and then they were dried over $MgSO_4$, filtered and concentrated under reduced pressure. The residue was then purified by flash chromatography (hexanes-AcOEt, 4:1 v/v) affording the desired compounds **8a-c**.

1-(4-Chlorophenyl)-2,5-dimethyl-1H-pyrrole-3-carbaldehyde (8a). Tan oil. R_f 0.67 (hexane/AcOEt 9:1). ^{1}H NMR (400 MHz $CDCl_3$) δ 9.71 (s, 1H), 7.41-7.39 (d, 2H, J =7.8), 7.10-7.07 (d, 2H, J =7.8), 6.25 (s, 1H), 2.17 (s, 3H), 1.88 (s, 3H) ppm. ^{13}C NMR (100 MHz $CDCl_3$) δ 185.3, 162.6, 138.7, 135.5, 130.9, 129.6, 129.3, 122.1, 106.15, 12.7, 11.2 ppm. Data are in agreement with those previously reported.[18]

1-(4-Fluorophenyl)-2,5-dimethyl-1H-pyrrole-3-carbaldehyde (8b). Tan oil. R_f 0.71 (hexane/AcOEt 9:1). ^{1}H NMR (400 MHz $CDCl_3$) δ 9.86 (s, 1H), 7.20-7.17 (m, 4H), 6.36 (s, 1H),

2.26 (s, 3H), 1.96 (s, 3H) ppm. ^{13}C NMR (100 MHz $CDCl_3$) δ 187.3, 129.8, 120.4, 117.2, 116.8, 116.6, 105.9, 12.7, 11.2 ppm. Data are in agreement with those previously reported.[18]

1,5-Bis(4-chlorophenyl)-2-methyl-1H-pyrrole-3-carbaldehyde (8c). White solid, mp 110 ºC. R_f 0.6 (hexane/AcOEt 1:1). ^{1}H NMR (400 MHz $CDCl_3$) δ 9.89 (s, 1H), 7.33 (d, 2H, J = 12 Hz), 7.09 (d, 2H, J = 12 Hz), 7.01 (d, 2H, J = 12 Hz), 6.87 (d, 2H, J = 12 Hz), 6.70 (s, 1H), 2.32 (s, 3H) ppm. ^{13}C NMR (100 MHz $CDCl_3$) δ 185.6, 140.1, 135.6, 134.5, 133.2, 132.0, 130.0, 129.8, 129.5, 129.4, 128.6, 122.9, 108.9, 11.5 ppm. LRMS m/z (ES+) m/z: 331 $[M+H]^+$.

Synthesis of pyrrole derivatives 9a-j. General Procedure.

The appropriate aldehyde **8a-c** (1 mmol) was dissolved in 5 mL of THF in a round bottom flask. Then AcOH (1 mmol) and the appropriate amine (1 mmol) were added to the stirring solution at room temperature. The mixture was allowed to stir at room temperature for 20 minutes before $NaB(AcO)_3H$ (3 mmol) was added. The mixture was allowed to stir at room temperature for 18h. Then, after completion, the reaction was quenched with NaOH 1M solution (25 mL). The mixture was then allowed to stir for 30 minutes. The reaction mixture was then diluted with EtOAc (10 mL), washed two times with EtOAc (10 mL) and once with brine (20 mL). The organic extracts were collected and then dried over $MgSO_4$, filtered and concentrated under reduced pressure. The residue was then purified by flash chromatography (hexane-AcOEt, 6:4 v/v) affording the desired compounds **9a-j**.

***N*-((1-(4-Chlorophenyl)-2,5-dimethyl-1H-pyrrol-3-yl)methyl)-2-phenylethan-1-amine (9a).** Tan oil. R_f 0.29 (AcOEt/hexane 1:1). ^{1}H NMR (400 MHz $CDCl_3$) δ 7.42-7.40 (d, 2H, J = 1.4 Hz), 7.29-7.27 (m, 2H), 7.24-7.22 (m, 3H), 7.12-7.10 (d, 2H, J = 1.4 Hz), 5.90 (s, 1H), 3.63 (s, 2H), 2.95 (m, 2H), 2.86 (m, 2H), 1.99 (s, 3H), 1.94 (s, 3H) ppm. ^{13}C NMR (100 MHz $CDCl_3$)

δ 140.3, 137.6, 133.5, 129.6, 129.3, 128.8, 128.5, 128.0, 126.1, 125.5, 118.1, 107.1, 51.0, 45.7, 36.4, 12.8, 10.7 ppm. LRMS m/z (ES+) m/z: 339 $[M+H]^+$. HRMS (ESI): calcd for $C_{21}H_{24}ClN_2$ ($M + H^+$) 339.1623, found 339.1603.

***N*-Benzyl-1-(1-(4-chlorophenyl)-2,5-dimethyl-1H-pyrrol-3-yl)methanamine (9b).** Tan oil. R_f 0.5 (AcOEt/hexane 1:1). ^{1}H NMR (400 MHz $CDCl_3$) δ 7.39 (d, 2H, J = 8.7 Hz), 7.34-7.27 (m, 4H), 7.22-7.20 (m, 1H), 7.10 (d, 2H, J = 8.7 Hz), 5.92 (s, 1H), 3.83 (s, 2H), 3.60 (s, 2H), 1.97 (s, 3H), 1.91 (s, 3H) ppm. ^{13}C NMR (100 MHz $CDCl_3$) δ 140.7, 137.6, 133.5, 129.6, 129.3, 128.3, 128.1, 127.9, 126.8, 125.6, 118.1, 107.1, 53.5, 45.0, 12.8, 10.7 ppm. LRMS m/z (ES+) m/z: 325 $[M+H]^+$. HRMS (ESI): calcd for $C_{20}H_{22}ClN_2$ ($M + H^+$) 325.1466, found 325.1466.

N-((1-(4-chlorophenyl)-2,5-dimethyl-1H-pyrrol-3-yl)methyl)cyclohexanamine (9c). Tan oil. R_f 0.17 (AcOEt/hexane 1:1). ^{1}H NMR (400 MHz $CDCl_3$) δ 7.40 (d, 2H, J = 8.2 Hz), 7.10 (d, 2H, J = 8.2 Hz), 5.91 (s, 1H), 3.59 (s, 2H), 2.53-2.48 (m, 1H), 1.98 (s, 3H), 1.95 (s, 3H), 1.94-1.90 (m, 2H), 1.74-1.70 (m, 2H), 1.16-1.06 (m, 3H), 0.85-0.81 (m, 3H) ppm. ^{13}C NMR (100 MHz $CDCl_3$) δ 137.6, 133.4, 129.6, 129.3, 128.0, 125.3, 118.6, 107.0, 56.7, 42.8, 33.6, 26.3, 25.1, 12.8, 10.7 ppm. LRMS m/z (ES+) m/z: 317 $[M+H]^+$. HRMS (ESI): calcd for $C_{19}H_{26}ClN_2$ ($M + H^+$) 317.1779, found 317.1779.

***N*-((1-(4-Chlorophenyl)-2,5-dimethyl-1H-pyrrol-3-yl)methyl)adamantan-2-amine (9d).** Tan oil. R_f 0.51 (AcOEt/hexane 1:1). ^{1}H NMR (400 MHz $CDCl_3$) δ 7.41 (d, 2H, J = 8.0 Hz), 7.12 (d, 2H, J = 8.0 Hz), 5.94 (s, 1H), 3.57 (s, 2H), 2.81 (m, 1H), 2.04-2.00 (m, 2H), 1.99 (s, 3H), 1.97 (s, 3H), 1.93 (m, 2H), 1.86-1.83 (m, 3H), 1.76-1.70 (m, 5H), 1.50-1.47 (m, 2H) ppm. ^{13}C NMR (100 MHz $CDCl_3$) δ 137.6, 133.4, 129.6, 129.3, 127.9, 125.4, 118.8, 107.2, 61.7, 42.9,

38.1, 37.7, 32.1, 31.5, 28.0, 27.8, 12.9, 10.7 ppm. LRMS m/z (ES+) m/z: 369 $[M+H]^+$. HRMS (ESI): calcd for $C_{23}H_{30}ClN_2$ ($M + H^+$) 369.2092, found 369.2089.

1-(1-(4-Chlorophenyl)-2,5-dimethyl-1H-pyrrol-3-yl)-N-(4-methylbenzyl)methanamine (9e). Tan oil. R_f 0.37 (AcOEt/MeOH 4:1). ^{1}H NMR (400 MHz $CDCl_3$) δ 7.41 (d, J = 8.7 Hz, 2H), 7.24 (d, J = 7.9 Hz, 2H), 7.13-7.10 (m, 4H), 5.94 (s, 1H), 3.18 (s, 2H), 3.61 (s, 2H), 2.32 (s, 3H), 1.99 (s, 3H), 1.93 (s, 3H), ppm. ^{13}C NMR (100 MHz $CDCl_3$) δ 137.6, 137.4, 136.4, 133.5, 129.6, 129.4, 129.1, 128.2, 128.0, 125.8, 117.9, 107.2, 53.1, 44.9, 21.2, 12.9, 10.8 ppm. LRMS m/z (ES+) m/z: 339 $[M+H]^+$. HRMS (ESI): calcd for $C_{21}H_{24}ClN_2$ ($M + H^+$) 339.1623, found 339.1624.

***N*-(4-Chlorobenzyl)-1-(1-(4-chlorophenyl)-2,5-dimethyl-1H-pyrrol-3-yl)methanamine (9f).** Tan oil. R_f 0.12 (AcOEt 100%). ^{1}H NMR (400 MHz $CDCl_3$) δ 7.41 (d, J = 8.7 Hz, 2H), 7.30-7.24 (m, 4H), 7.11 (d, J = 8.2 Hz, 2H), 5.91 (s, 1H), 3.81 (s, 2H), 3.59 (s, 2H), 1.99 (s, 3H), 1.92 (s, 3H) ppm. ^{13}C NMR (100 MHz $CDCl_3$) δ 139.3, 133.7, 129.6, 129.5, 129.4, 128.4, 128.1, 125.7, 117.9, 107.1, 52.7, 45.1, 12.8, 10.8 ppm. LRMS m/z (ES+) m/z: 359 $[M+H]^+$. HRMS (ESI): calcd for $C_{20}H_{21}Cl_2N_2$ ($M + H^+$) 359.1076, found 359.1076.

***N*-(4-Fluorobenzyl)-1-(1-(4-chlorophenyl)-2,5-dimethyl-1H-pyrrol-3-yl)methanamine (9g).** Tan oil. R_f 0.16 (AcOEt 100%). ^{1}H NMR (400 MHz $CDCl_3$) δ 7.41 (d, J= 8.7 Hz, 2H), 7.31 (dd, J = 8.7 Hz 2H), 7.11 (d, J = 8.2 Hz, 2H), 6.99 (t, J= 8.2 Hz, 2H), 5.91 (s, 1H), 3.81 (s, 2H), 3.59 (s, 2H), 1.99 (s, 3H), 1.92 (s, 3H) ppm. ^{13}C NMR (100 MHz $CDCl_3$) δ 163.1, 160.7, 137.6, 133.6, 129.7, 129.6, 129.4, 128.1, 125.7, 118.0, 115.2, 107.1, 52.8, 45.1, 12.8, 10.8 ppm. LRMS m/z (ES+) m/z: 343 $[M+H]^+$. HRMS (ESI): calcd for $C_{20}H_{21}ClFN_2$ ($M + H^+$) 343.1372, found 343.1374.

***N*-Benzyl-1-(1-(4-fluorophenyl)-2,5-dimethyl-1H-pyrrol-3-yl)methanamine (9h).** Tan oil. R_f 0.20 (AcOEt/hexane 4:1). ^{1}H NMR (400 MHz $CDCl_3$) δ 7.36-7.29 (m, 4H), 7.23 (t, *J* = 7.9 Hz, 1H), 7.15-7.09 (m, 4H), 5.92 (s, 1H), 3.85 (s, 2H), 3.61 (s, 2H), 1.98 (s, 3H), 1.91 (s, 3H) ppm. ^{13}C NMR (100 MHz $CDCl_3$) δ 130.1, 129.9, 128.4, 128.2, 117.9, 116.2, 115.9, 106.8, 53.6, 45.2, 12.9, 10.8 ppm. LRMS m/z (ES+) m/z: 309 $[M+H]^+$. HRMS (ESI): calcd for $C_{20}H_{22}FN_2$ ($M + H^+$) 309.1762, found 309.1764.

***N*-Benzyl-1-(1,5-bis(4-chlorophenyl)-2-methyl-1H-pyrrol-3-yl)methanamine (9i).** White solid, mp 183 ºC. R_f 0.23(AcOEt/MeOH 9:1). ^{1}H NMR (400 MHz $CDCl_3$) δ 7.31-7.25 (m, 7H), 7.04 (d, 2H, J = 12 Hz), 6.97 (d, 2H, J = 12 Hz), 6.86 (d, 2H, J = 12 Hz), 6.31 (s, 1H), 3.82 (s, 2H), 3.62 (s, 2H), 1.96 (s, 3H), 1.80 (brs, 1H) ppm. ^{13}C NMR (100 MHz $CDCl_3$) δ 137.3, 133.9, 132.7, 132.0, 130.0, 129.6, 129.5, 128.9, 128.3, 111.4, 110.5, 29.1, 24.6, 11.4 ppm. LRMS m/z (ES+) m/z: 421 $[M+H]^+$. HRMS (ESI): calcd for $C_{25}H_{23}Cl_2N_2$ ($M + H^+$) 421.1233, found 421.1228.

***N*-((1,5-Bis(4-chlorophenyl)-2-methyl-1H-pyrrol-3-yl)methyl)cyclohexanamine (9j).** White solid, mp 218 ºC. R_f 0.32(AcOEt/MeOH 9:1). ^{1}H NMR (400 MHz $CDCl_3$) δ 7.24 (d, 2H, J = 12 Hz), 7.00 (d, 2H, J = 12 Hz), 6.95 (d, 2H, J = 12 Hz), 6.80 (d, 2H, J = 12 Hz), 6.69 (s, 1H), 2.93-2.87 (m, 1H), 2.19 (d, 2H, J = 12 Hz), 2.01 (s, 3H), 1.76-1.63 (m, 3H), 1.21-1.15 (m, 3H) ppm. ^{13}C NMR (100 MHz $CDCl_3$) δ 137.0, 133.9, 132.0, 129.7, 128.9, 128.3, 111.4, 110.5, 55.0, 39.4, 29.1, 28.9, 24.6, 11.4 ppm. LRMS m/z (ES+) m/z: 413 $[M+H]^+$. HRMS (ESI): calcd for $C_{24}H_{27}Cl_2N_2$ ($M + H^+$) 413.1546, found 413.1548.

Synthesis of oximes 10a-b. General procedure.[18]

The appropriate aldehyde **8a-b** (1 mmol) was dissolved in 5mL of THF in a round bottom flask. Then AcOH (1 mmol) and benzyl-hydroxylamine (1 mmol) were added to the stirring solution at room temperature. The mixture was allowed to stir at room temperature for 18h. After completion, the reaction was quenched with NaOH 1M solution (25 mL). The reaction mixture was then diluted with EtOAc (10 mL), washed two times with EtOAc (10 mL) and once with brine (20 mL). The organic extracts were collected and then dried over $MgSO_4$, filtered and concentrated under reduced pressure. The residue was then purified by flash chromatography (hexanes-AcOEt, 6:4 v/v) affording the desired compounds **10a-b**.

1-(4-Chlorophenyl)-2,5-dimethyl-1H-pyrrole-3-carbaldehyde O-benzyl oxime (10a). Tan oil. R_f 0.88 (hexane/Et_2O 3:2). ^{1}H NMR (400 MHz $CDCl_3$) δ 8.15, 7.45-7.41 (m, 4H), 7.37-7.33 (m, 2H), 7.30-7.29 (m, 1H), 7.11 (d, 2H, J = 8.7 Hz), 6.24 (s, 1H), 5.14 (s, 2H), 2.03 (s, 3H), 1.97 (s, 3H) ppm. ^{13}C NMR (100 MHz $CDCl_3$) δ 144.6, 138.0, 136.6, 134.3, 130.8, 130.1, 129.7, 129.6, 128.5, 128.4, 127.8, 112.9, 104.6, 75.9, 12.8, 11.5 ppm. LRMS m/z (ES+) m/z: 339 $[M+H]^+$. HRMS (ESI): calcd for $C_{20}H_{19}ClN_2O$ ($M + H^+$) 339.1259, found 339.1260.

Synthesis of compounds 11a-b. General procedure.

The appropriate oxime **10a-b** (1 mmol) was dissolved in 5 mL of THF in a round bottom flask. Then, $NaBH_3(CN)$ (3 mmol) was added to the solution and the mixture was allowed to stir at room temperature for 18h. Then, the reaction was quenched with NaOH 1M solution (25 mL). The reaction mixture was then diluted with EtOAc (10 mL), washed two times with EtOAc (10 mL) and once with brine (20 mL). The organic extracts were collected and then it was dried over $MgSO_4$, filtered and concentrated under reduced pressure. The residue was then purified by flash chromatography (hexanes-AcOEt, 6:4 v/v) affording the desired compounds **11a-b**.

O-Benzyl-*N*-((1-(4-chlorophenyl)-2,5-dimethyl-1H-pyrrol-3-yl)methyl)hydroxylamine (11a). Tan oil. R_f 0.43 (AcOEt/hexane 2:3). ^{1}H NMR (400 MHz $CDCl_3$) δ 7.42-7.25 (m, *7*H), 7.10 (d, 2H, *J* = 8.7 Hz), 5.90 (s, 1H), 5.48 (brs, 1H), 4.74 (s, 2H), 3.91 (s, 2H), 1.97 (s, 3H), 1.93 (s, 3H) ppm. ^{13}C NMR (100 MHz $CDCl_3$) δ 138.2, 137.5, 133.6, 129.6, 129.4, 128.6, 128.4, 128.2, 127.3, 126.9, 114.3, 107.6, 76.1, 48.5, 12.8, 10.7 ppm. LRMS m/z (ES+) m/z: 339 [M-H^+]. HRMS (ESI): calcd for $C_{20}H_{20}ClN_2O$ (M - H^+) 339.1264, found 339.1259.

O-Benzyl-*N*-((1-(4-fluorophenyl)-2,5-dimethyl-1H-pyrrol-3-yl)methyl)hydroxylamine (11b). R_f 0.45 (AcOEt/hexane 2:3). Tan oil. ^{1}H NMR (400 MHz $CDCl_3$) δ 7.39-7.28 (m, 5H), 7.12 (m, 4H), 5.90 (s, 1H), 4.75 (s, 2H), 3.92 (s, 2H), 1.96 (s, 3H), 1.92 (s, 3H) ppm. ^{13}C NMR (100 MHz $CDCl_3$) δ 138.2, 134.9, 130.0, 129.9, 128.6, 128.4, 128.3, 127.8, 127.1, 116.2, 115.9, 114.0, 107.3, 76.1, 48.5, 12.8, 10.7 ppm. LRMS m/z (ES+) m/z: 323 [M - H^+]. HRMS (ESI): calcd for $C_{20}H_{20}FN_2O$ (M - H^+) 323.1560, found 323.1554.

AUTHOR INFORMATION

Corresponding Authors

*daniele.castagnolo@kcl.ac.uk; Tel. +44(0)2078484506

*fabrizio.manetti@unisi.it; Tel. +390577234256

PRESENT ADDRESS

‡Current address: The Francis Crick Institute, Mill Hill Laboratory, The Ridgeway, Mill Hill, London, NW7 1AA, UK.

AUTHOR CONTRIBUTION

The manuscript was written and enhanced through contributions of all authors. All authors have given approval to the final version of the manuscript. ¶These authors contributed equally.

SUPPORTING INFORMATION

Copies of ^{1}H NMR and ^{13}C NMR spectra for compounds **7g**, **7j**, **9a**, **9b**, **9c**

ABBREVIATIONS USED

MTB, *Mycobacterium tuberculosis*; MDR-TB, multidrug-resistant tuberculosis; XDR-TB, extensively drug-resistant tuberculosis; TDR-TB, Totally drug-resistant tuberculosis; MmpL, mycobacterial membrane protein large; RND, resistance-nodulation-cell division; BCG, bacille Calmette-Guerin; GIC_{50}, 50% growth inhibitory concentration; SI, selectivity index; EPI, efflux pump inhibitory; ADC, albumin-dextrose-catalase; OADC, oleic acid-albumin-dextrose-catalase; CFU, colony forming unit; MABA, Microplate Alamar Blue assay; FBS, Fetal bovine serum; OD600, Optical density 6000.

FUNDING SOURCES

Medical Research Council grant (G0801956), Wellcome Trust/Birkbeck Anniversary Scholarship and Birkbeck Translational Research Award. Royal Society of Chemistry (Research Fund 2015) and Northumbria University PhD Studentship. The funders had no role in study design, data collection and analysis, decision to publish, or preparation of the manuscript.

ACKNOWLEDGMENT

We gratefully acknowledge the EPSRC UK National Mass Spectrometry Facility for providing the mass spectrometry data. Professor A. Tafi is also acknowledged for helpful discussion on the computational details. AM is a Birkbeck Anniversary/ Wellcome Trust Scholar, SB is a Cipla Distinguished Fellow in Pharmaceutical Sciences. DC thanks the Royal Society of Chemistry for financial support (Research Fund 2015).

REFERENCES

1. WHO. Global tuberculosis report 2015. http://www.who.int/tb/publications/global_report/en/ (accessed February 08th, 2016).

2. Caminero, J. A. Treatment of multidrug-resistant tuberculosis: evidence and controversies. *Int. J. Tuberc. Lung Dis.* **2006**, *10*, 829–837.

3. Chan, E. D.; Laurel, V.; Strand, M. J.; Chan, J. F.; Huynh, M. L.; Goble, M.; Iseman, M. D. Treatment and outcome analysis of 205 patients with multidrug-resistant tuberculosis. *Am. J. Respir. Crit. Care Med.* **2004**, *169*, 1103–1109.

4. Eker, B.; Ortmann, J.; Migliori, G. B.; Sotgiu, G.; Muetterlein, R.; Centis, R.; Hoffmann, H.; Kirsten, D.; Schaberg, T.; Ruesch-Gerdes, S.; Lange, C. Multidrug- and extensively drug-resistant tuberculosis, Germany. *Emerging Infect. Dis.* **2008**, *14*, 1700–1706.

5. Mitnick, C.D.; Shin, S. S.; Seung, K. J.; Rich, M. L.; Atwood, S.S.; Furin, J. J.; Fitzmaurice, G. M.; Alcantara Viru, F. A.; Appleton, S. C.; Bayona, J. N.; Bonilla, C. A.; Chalco, K.; Choi, S.; Franke, M. F.; Fraser, H. S.; Guerra, D.; Hurtado, R. M.; Jazayeri, D.;

Joseph, K.; Llaro, K.; Mestanza, L.; Mukherjee, J. S.; Muñoz, M.; Palacios, E.; Sanchez, E.; Sloutsky, A.; Becerra, M. C. Comprehensive treatment of extensively drug-resistant tuberculosis. *N. Engl. J. Med.* **2008**, *359*, 563–574.

6. Migliori, G. B.; Loddenkemper, R.; Blasi, F.; Raviglione, M. C. 125 years after Robert Koch's discovery of the tubercle bacillus: the new XDR-TB threat. Is "science" enough to tackle the epidemic? *Eur. Respir. J.* **2007**, *29*, 423-427.

7. Velayati, A. A.; Farnia, P.; Masjedi, M. R. The totally drug resistant tuberculosis (TDR-TB). *Int. J. Clin. Exp. Med.* **2013**, *6*, 307–309.

8. Biava, M.; Porretta, G.C.; Poce, G.; Supino, S.; Deidda, D.; Pompei, R.; Molicotti, P.; Manetti, F.; Botta, M. Antimycobacterial agents. Novel diarylpyrrole derivatives of BM212 endowed with high activity toward *Mycobacterium tuberculosis* and Low Cytotoxicity. *J. Med. Chem.* **2006**, *49*, 4946-4952.

9. Alfonso, S. BM212-derived MmpL3 inhibitors enabling new possibilities for the treatment of TB and studies of mycobacterial iron assimilation as new potential target for drug discovery. *PhD Thesis*, Sapienza Università di Roma, September 10, **2013**, http://hdl.handle.net/10805/2145, accessed April 27, 2015.

10. Biava, M.; Porretta, G.C.; Poce, G.; Battilocchio, C.; Alfonso, S.; de Logu, A.; Manetti, F.; Botta, M. Developing pyrrole-derived antimycobacterial agents: a rational lead optimization approach. *ChemMedChem* **2011**, *6*, 593-599.

11. Poce, G.; Bates, R.H.; Alfonso, S.; Cocozza, M.; Porretta, G.C.; Ballell, L.; Rullas, J.; Ortega, F.; De Logu, A.; Agus, E.; La Rosa, V.; Pasca, M.R.; De Rossi, E.; Wae, B.;

Franzblau, S.G.; Manetti, F.; Botta, M.; Biava, M. Improved BM212 MmpL3 inhibitor analogue shows efficacy in acute murine model of tuberculosis infection. *PLoS One* **2013**, *8*, e56980.

12. Lun, S.; Guo, H,; Onajole, O. K.; Pieroni, M,; Gunosewoyo, H.; Chen, G.; Tipparaju, S. K.; Ammerman, N. C.; Kozikowski, A. P.; Bishai, W. R. Indoleamides are active against drug-resistant Mycobacterium tuberculosis. *Nat. Commun.* **2013**, *4*, 2907.

13. La Rosa, V.; Poce, G.; Canseco, J.O.; Buroni, S.; Pasca, M.R.; Biava, M.; Raju, R.M.; Porretta, G.C.; Alfonso, S.; Battilocchio, C.; Javid, B.; Sorrentino, F.; Ioerger, T.R.; Sacchettini, J.C.; Manetti, F.; Botta, M.; De Logu, A.; Rubin, E.J.; De Rossi, E. MmpL3 is the cellular target of the antitubercular pyrrole derivative BM212. *Antimicrob. Agents Chemother.* **2012**, *56*, 324-331.

14. Protopopova, M.; Hanrahan, C.; Nikonenko, B.; Samala, R.; Chen, P.; Gearhart, J.; Einck, L.; Nacy, C. A. Identification of a new antitubercular drug candidate, SQ109, from a combinatorial library of 1,2-ethylenediamines. *J. Antimicrob. Chemother.* **2005**, *56*, 968-974.

15. Nikonenko, B. V.; Protopopova, M.; Samala, R.; Einck, L.; Nacy, C. A. Drug therapy of experimental tuberculosis (TB): improved outcome by combining SQ109, a new diamine antibiotic, with existing TB drugs. *Antimicrob. Agents Chemother.* **2007**, 51, 1563–1565.

16. Jia, L.; Tomaszewski, J.E.; Hanrahan, C.; Coward, L.; Noker, P.; Gorman, G.; Nikonenko, B.; Protopopova, M. Pharmacodynamics and pharmacokinetics of SQ109, a new diamine-based antitubercular drug. *Br. J. Pharmacol.* **2005**, *144*, 80-87.

17. Heinrich, N.; Dawson, R.; du Bois, J.; Narunsky, K.; Horwith, G.; Phipps, A. J.; Nacy, C. A.; Aarnoutse, R. E.; Boeree, M. J.; Gillespie, S. H.; Venter, A.; Henne, S.; Rachow, A.; Phillips, P. P.; Hoelscher, M.; Diacon, A. H. Early phase evaluation of SQ109 alone and in combination with rifampicin in pulmonary TB patients. *J. Antimicrob. Chemother.* **2015**, *70*, 1558-1566.

18. Manetti, F.; Magnani, M.; Castagnolo, D.; Passalacqua, L.; Botta, M; Corelli, F.; Saddi, M.; Deidda, D.; De Logu, A. Ligand-based virtual screening, parallel solution-phase and microwave-assisted synthesis as tools to identify and synthesize new inhibitors of mycobacterium tuberculosis. *ChemMedChem* **2006**, *1*, 973-989.

19. Badiola, K. A.; Quan, D. H.; Triccas, J. A.; Todd, M. H. Efficient synthesis and anti-tubercular activity of a series of spirocycles: an exercise in open science. *PLoS One* **2014**, *9*, e111782.

20. *Phase*, version 3.3, Schrodinger LLC., NY, 2011.

21. Wermuth, C. G., Aldous, D., Raboisson, P., Rognan, D., Eds.; *The Practice of Medicinal Chemistry*, 4th ed.; Academic Press: London, 2015; p 385.

22. Ritchie, T. J.; Macdonald, S. J.; Young, R. J.; Pickett, S. D. The impact of aromatic ring count on compound developability: further insight by examining carbo- and hetero-aromatic and –aliphatic ring types. *Drug Discovery Today* **2011**, *16*, 164-171

23. Castagnolo, D.; De Logu, A.; Radi, M.; Bechi, B.; Manetti, F.; Magnani, M.; Supino, S.; Meleddu, R.; Chisu, L.; Botta, M. Synthesis, biological evaluation and SAR study of novel

pyrazole analogues as inhibitors of *Mycobacterium tuberculosis*. *Bioorg. Med. Chem.* **2008**, *16*, 8587-8591.

24. Castagnolo, D.; Manetti,F.; Radi,M.; Bechi, B.; Pagano,M.; De Logu,A.; Meleddu, R.; Saddi, M.; Botta, M. Synthesis biological evaluation and SAR study of novel pyrazole analogues as inhibitors of *Mycobacterium tuberculosis*: Part 2. Synthesis of rigid pyrazolones. *Bioorg. Med. Chem.* **2009**, *17*, 5716-5721.

25. Phelan, J.; Maitra, A.; McNerney, R.; Nair, M.; Gupta, A.; Coll, F.; Pain, A.; Bhakta, S.; Clark, T.G. The draft genome of *Mycobacterium aurum*, a potential model organism for investigating drugs against *Mycobacterium tuberculosis* and *Mycobacterium leprae*. *Int. J. Mycobacteriology* **2015**, *4*, 207-216.

26. Naik, S. K.; Mohanty, S.; Padhi, A.; Pati, R.; Sonawane, A. Evaluation of antibacterial and cytotoxic activity of *Artemisia nilagirica* and *Murraya koenigii* leaf extracts against mycobacteria and macrophages. *BMC Complementary Altern. Med.* **2014**, *14*, 87.

27. Gupta, A.; Bhakta, S. An integrated surrogate model for screening of drugs against *Mycobacterium tuberculosis*. *J. Antimicrob. Chemother.* **2012**, *66*, 1380-1391.

28. *Maestro*, version 9.2, Schrodinger LLC., NY, 2011.

29. *MacroModel*, version 9.9, Schrodinger LLC., NY, 2011.

30. Sambandamurthy, V. K.; Derrick, S. C.; Hsu, T.; Chen, B.; Larsen, M. H.; Jalapathy, K. V.; Chen, M.; Kim, J.; Porcelli, S. A.; Chan, J.; Morris, S. L.; Jacobs, W. R. Jr. *Mycobacterium tuberculosis* DeltaRD1 DeltapanCD: a safe and limited replicating mutant

strain that protects immunocompetent and immunocompromised mice against experimental tuberculosis. *Vaccine* **2006**, *24*, 6309-6320.

31. Larsen, M. H.; Biermann, K.; Chen, B.; Hsu, T.; Sambandamurthy, V. K.; Lackner, A. A.; Aye, P. P.; Didier, P.; Huang, D.; Shao, L.; Wei, H.; Letvin, N. L.; Frothingham, R.; Haynes, B. F.; Chen, Z. W.; Jacobs, Jr. W. R. Efficacy and safety of live attenuated persistent and rapidly cleared *Mycobacterium tuberculosis* vaccine candidates in non-human primates. *Vaccine* **2009**, *27*, 4709-4717.

32. Sambandamurthy, V. K.; Wang, X.; Chen, B.; Russell, R. G.; Derrick, S.; Collins, F. M.; Morris, S. L.; Jacobs Jr. W. R. A pantothenate auxotroph of Mycobacterium tuberculosis is highly attenuated and protects mice against tuberculosis. *Nat. Med.* **2002**, *8*, 1171–1174.

33. Evangelopoulos, D. and Bhakta, S. Rapid methods for testing inhibitors of mycobacterial growth. *Methods Mol. Biol.* **2010**, *642*, 193-201

34. Guzman, J. D.; Evangelopoulos, D.; Gupta, A.; Birchall, K.; Mwaigwisya, S.; Saxty, B.; McHugh, T. D.; Gibbons, S.; Malkinson, J.; Bhakta, S. Antitubercular specific activity of ibuprofen and the other 2-arylpropanoic acids using the HT-SPOTi whole-cell phenotypic assay. *BMJ Open* **2013**, *3*, e002672.

35. Danquah, C. A.; Maitra, A.; Gibbons, S.; Faull, J.; Bhakta, S. HT-SPOTi: a rapid, drug susceptibility test (DST), to evaluate antibiotic resistance profiles and novel chemicals for anti-infective drug discovery. *Curr. Protoc. Microbiol.* **2016**, *40*, 17-18.

36. Rodrigues, L.; Wagner, D.; Viveiros, M.; Sampaio, D.; Couto, I.; Vavra, M.; Kern, W. V.; Amaral, L. Thioridazine and chlorpromazine inhibition of ethidium bromide efflux in

Mycobacterium avium and *Mycobacterium smegmatis*. *J. Antimicrob. Chemother.* **2008**, *61*, 1076-1082.

FIGURES

Figure 1. Graphical representation (left) of **1** and **2**, and rough comparison of the topological distribution of their chemical features (middle upper panel), and superposition of their three-dimensional conformers as generated by the common feature hypothesis generation routine (middle lower panel; **1**: blue, **2**: red). The flexible structure of **2** is well superposable to the skeleton of **1**. The general structures **A** and **B** of the hybrid compounds are also shown (right).

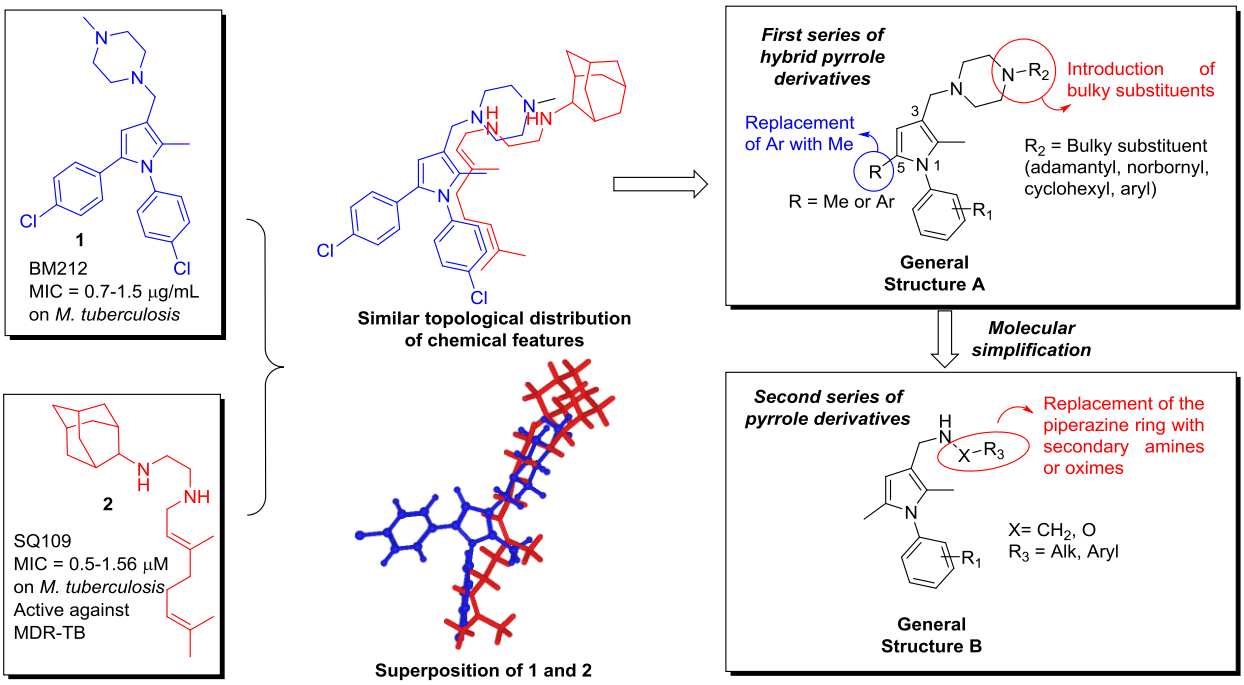

Figure 2. Graphical representation of the four-feature superposition model common to **1** (thin lines) and **2** (thick lines). The two protonatable chemical features (P7 and P8) are in blue, while the two hydrophobic regions (H4 and H6) are in green. The conformer of **1** represented in the picture is 0.013 kJ/mol far from the lowest energy conformation, while the energy difference between the lowest energy conformation of **2** and the conformer reported in the picture is 4.660 kJ/mol.

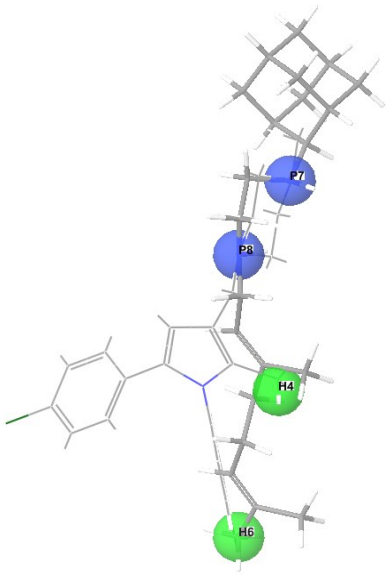

Figure 3. Graphical representation of the four-feature improved model matched by the most active hybrid pyrrole **9c**. Changes occurred within the region of space occupied by the C3 side chain: the positively ionized P8 feature previously accommodating the N4 nitrogen atom of the piperazine was omitted, while an additional hydrophobic region was added, that corresponded to the terminal bulky substituent of the C3 side chain.

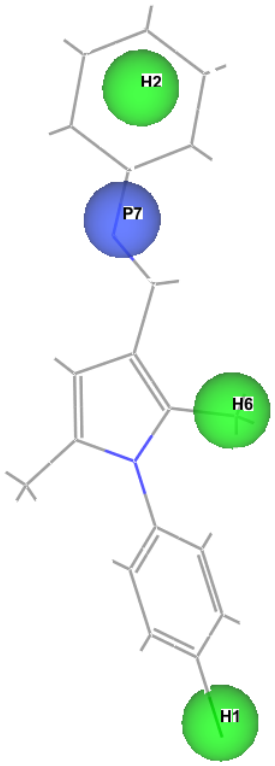

SCHEMES

Scheme 1. Synthesis of pyrroles **3a-e** and piperazines **6a-b**

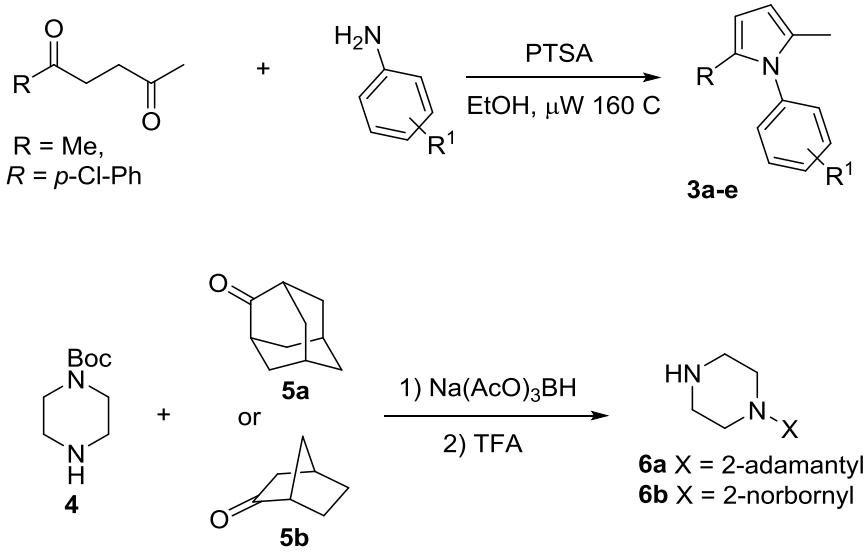

Scheme 2. Synthesis of pyrroles **9**, **10** and **11**

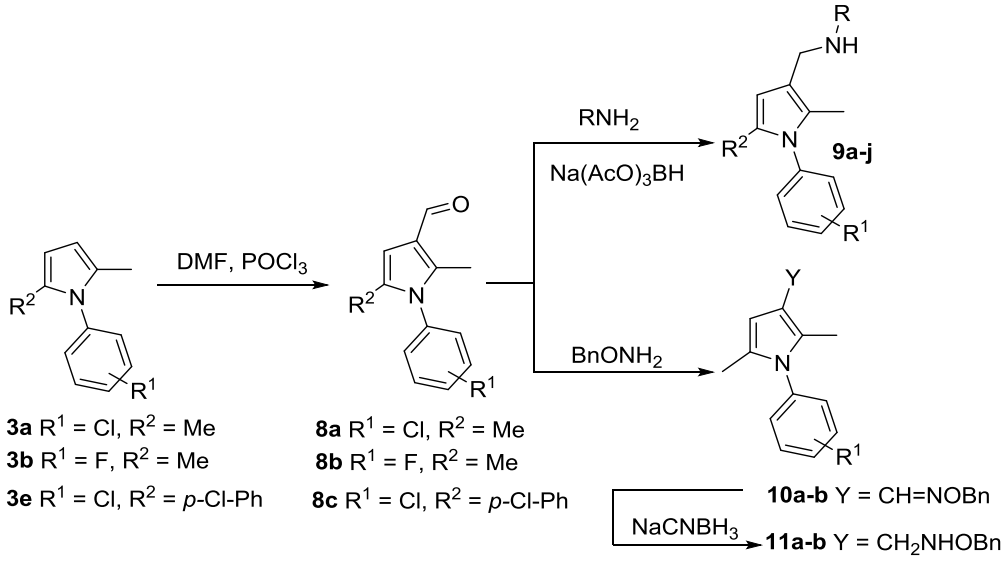

TABLES.

Table 1. First series of pyrrole derivatives **7a-l**

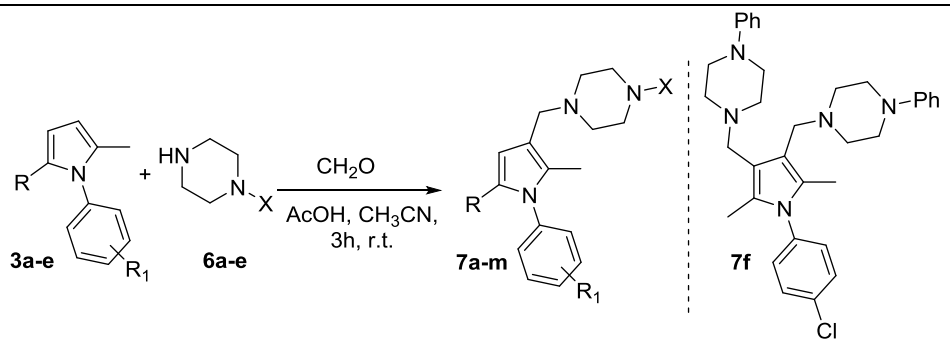

Cmpd	R	R^1	X	Yield %[a]
7a	Me	4-Cl	2-Adamantyl	56
7b	Me	2-F	2-Adamantyl	45
7c	Me	4-iPr	2-Adamantyl	51
7d	Me	3-Me	2-Adamantyl	48
7e	Me	4-Cl	Phenyl	65
7f[b]	Me	4-Cl	Phenyl	35
7g	Me	4-Cl	2-Norbornyl[c]	55
7h	Me	4-Cl	Cyclohexyl	52
7i	Me	4-Cl	1-Adamantyl	54
7j	4-Cl-Phenyl	4-Cl	Phenyl	64
7k	4-Cl-Phenyl	4-Cl	2-Adamantyl	65
7l	4-Cl-Phenyl	4-Cl	1-Adamantyl	60
7m	4-Cl-Phenyl	4-Cl	2-Norbornyl[c]	56

[a]Isolated yields are reported. [b]Isolated as side product. [c]Mixture of exo/endo isomers.

Table 2. Second series of pyrrole derivatives

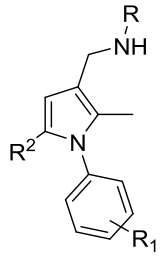

9a-j

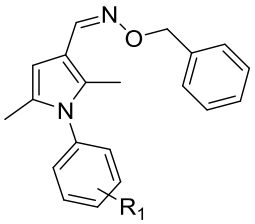

10a-b

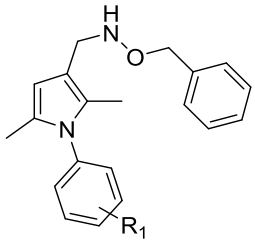

11-ab

Cmpd	R^1	R^2	R	Yield %[a]
9a	Cl	Me	$PhCH_2CH_2$	75
9b	Cl	Me	$PhCH_2$	79
9c	Cl	Me	Cyclohexyl	77
9d	Cl	Me	2-Adamantyl	60
9e	Cl	Me	4-Me-Bn	82
9f	Cl	Me	4-Cl-Bn	78
9g	Cl	Me	4-F-Bn	80
9h	F	Me	$PhCH_2$	82
9i	Cl	4-Cl-Phenyl	$PhCH_2$	78
9j	Cl	4-Cl-Phenyl	Cyclohexyl	75
10a	Cl	-	-	75
10b[15]	F	-	-	78
11a	Cl	-	-	80
11b	F	-	-	82

[a]Isolated yields

Table 3. Anti-tubercular activity on *M. smegmatis*, *M. bovis* BCG and *M. aurum* mycobacterial strains.

Cmpd	MIC (μg/mL)		
	***M. smegmatis* mc^{2}155**	***M. bovis* BCG**	***M. aurum***
7a	8.0	3.3	7.8
7b	13	1.3	250
7c	21	4.0	500
7d	64	62	500
7e	32	32	31
7f	>64	>64	250
7g	27	32	16
7h	27	21	31
7i	8.0	16	16
7j	>64	2.0	-
7k	>64	64	-
7l	3.3	2.0	62
7m	64	64	250
9a	32	16	16
9b	4.0	0.5	1.9
9c	8.0	0.4	7.8
9d	16	2.0	62
9e	8.0	4.0	1.9
9f	4.0	8.0	1.9

9g	2.0	0.5	1.9
9h	16	13	7.8
9i	8.0	8.0	1.0
9j	4.0	4.0	1.0
10a	>64	>64	-
11a	>64	>64	-
11b	>64	>64	-
1	25[8]	0.78[11]	16
2	4	2	7.8

'-' indicates that no inhibition was seen even at the maximum concentration tested in the experiment (125 µg/mL in the case of *M. smegmatis* and *M. bovis* BCG and 500 µg/mL in the case of *M. aurum*). All experiments have been performed in triplicate.

Table 4. Biological evaluation of the compounds against bacterial and eukaryotic cells. Selectivity index (SI) is calculated as the ratio between *M. tuberculosis* H37Rv MIC and GIC_{50}.

Cmpd	*M. tuberculosis* MIC (μg/mL)				GIC_{50} (μg/mL)	GIC_{50} (μg/mL)	SI	SI
	$mc^2$7000	H37Rv	MDR1	MDR2	RAW 264.7	THP-1	RAW 264.7	THP-1
7a	3.3	7.8	7.8	16	5.7	32 ± 1	0.7	4.1
7b	1.0	3.9	7.8	16	11	26 ± 1	2.8	6.7
7c	3.3	16	62	125	92	72 ± 1	5.7	4.5
7d	32	16	31	125	22	37 ± 1	1.4	2.3
7e	32	7.8	31	>125	33	25 ± 1	4.2	3.2
7f	>64	31	62	>125	500	113 ± 1	16	3.6
7g	2.0	1.9	3.9	31	5.6	16 ± 5	2.9	8.4
7h	8.0	3.9	7.8	62	5.5	16 ± 1	1.4	4.1
7i	8.0	16	125	125	0.1	16 ± 1	0.006	1.0
7j	1.0	1.9	3.9	>125	175	294 ± 5	92	155
7k	>64	62	125	125	95	500 ± 10	1.5	8.1
7l	0.5	7.8	16	62	23	35 ± 18	2.9	4.5
7m	64	-	-	-	-	429	-	6.7
9a	4.0	1.0	1.9	7.8	9.9	7.3 ± 2.7	10	7.3
9b	0.5	0.5	1.0	3.9	5.5	7.2 ± 3.7	11	14
9c	0.5	0.2	0.5	16	10	7.4 ± 1.4	50	37
9d	1.0	1.9	3.9	125	19	15 ± 10	10	7.8
9e	2.0	1.0	3.9	7.8	0.1	6.1 ± 2.1	0.1	6.1
9f	2.0	16	31	>125	0.1	18 ± 1	0.006	1.1

9g	0.7	>125	-	16	26	8.4 ± 1.7		
9h	4.0	1.0	7.8	62	5.6	28 ± 1	5.6	28
9i	16	-	-	-	-	99 ± 1	-	6.1
9j	8	-	-	-	-	3.9	-	0.5
10a	>64	>125	>125	>125	128	500 ± 22	≅1	<4
10b	-	25[15]	-	-	-		-	-
11a	>64	-	125	-	133	67 ± 1	-	-
11b	>64	>125	62	>125	123	292 ± 41	≅1	<2.3
1	8	1.0	3.9	16	19	3.23[11]	19	3.23
2	2	0.51[15]	ND	ND	ND	-	ND	ND
INH	-	0.24	10	25	ND	-	ND	-

ND: not determined. '-' indicates that no inhibition was seen even at the maximum concentration tested in the experiment (125 µg/mL in the case of *M. tuberculosis* variants). Isoniazid (INH) was used as drug control. All experiments have been performed in triplicate.

Figure 4. Graphs showing the accumulation of ethidium bromide (EtBr) within *M. aurum* cells in the presence of selected compounds and positive (Verapamil) and negative (1x PBS) controls. Low to very high inhibition of efflux (as a representation of increased level of EtBr accumulation) are shown by the numbers 1-4. The experiments were performed in triplicate (n=3) and the graph is plotted using the average values obtained.

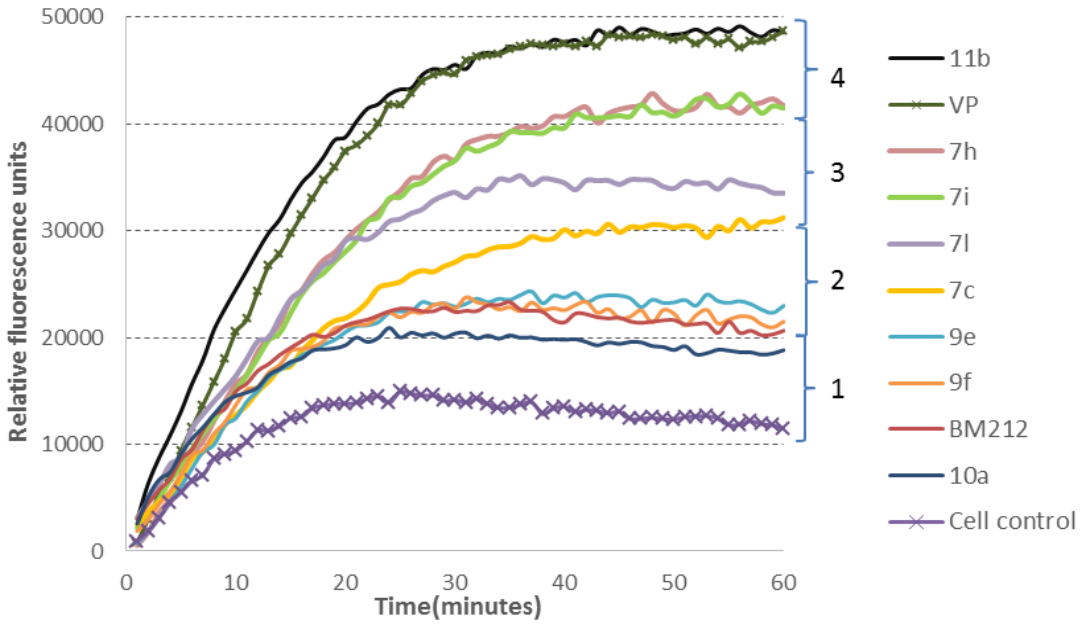

Table 5. Efflux pump inhibitory (EPI) activity.

Cmpd	EPI *M. aurum*	Cmpd	EPI *M. aurum*	Cmpd	EPI *M. aurum*
7a	1	**7k**	0	**9h**	1
7b	1	**7l**	3	**9i**	1
7c	3	**7m**	ND	**9j**	2
7d	2	**9a**	2	**10a**	1
7e	1	**9b**	2	**10b**	ND
7f	2	**9c**	2	**11a**	2
7g	1	**9d**	1	**11b**	4
7h	4	**9e**	2	**1**	2
7i	4	**9f**	2	**2**	2
7j	2	**9g**	1	**INH**	ND

Efflux pump inhibitory (EPI) activity of the compounds is marked from 0-4 wherein: 0 refers to no inhibition, 1-low inhibition (efflux substrate accumulation above cell control to 20,000 relative fluorescence units), 2-moderate inhibition (efflux substrate accumulation between 20-30,000 units), 3-high inhibition (efflux substrate accumulation between 30-40,000 units), 4-very high inhibition (efflux substrate accumulation between 40-50,000 units). ND: not determined.

Insert Table of Contents Graphic and Synopsis Here